Alejandra Febus Gonzalez

Cloning and Preliminary Functional Analysis of Zebrafish BiP, an ATPase-Dependent Endoplasmic Reticulum Chaperone

UNIVERSIDADE DO ALGARVE

Faculdade de Ciências e Tecnologia

2025

Mestrado em Biologia Marinha

Supervisors:

Eduardo José Xavier Rodrigues de Pinho e Melo

Statements of authorship and copyright

I, Alejandra Febus Gonzalez, declare that this thesis titled "Cloning and Preliminary Functional Analysis of Zebrafish BiP, an ATPase-Dependent Endoplasmic Reticulum Chaperone" and the work presented in it are my own and have been generated by me as the result of my own original research.

I confirm that: This work has not been submitted in whole or in part for any other degree or qualification. Where information has been derived from other sources, I confirm that this has been clearly indicated and acknowledged. All experimental work, data interpretation, and written analysis presented are my own unless otherwise stated. I retain the copyright of this thesis and grant permission for it to be made available to the public in accordance with the policies of Universidade do Algarve. Reproduction of any part of this thesis for scholarly purposes is permitted, provided that proper acknowledgment is given.

Abstracts

Title: *Molecular Cloning and Preliminary Functional Characterization of Zebrafish BiP Chaperone*

The endoplasmic reticulum chaperone BiP (Binding immunoglobulin Protein) plays a fundamental role in protein homeostasis, mediated by its ATPase activity. To investigate the evolutionary conservation and functionality of BiP in vertebrates, we cloned the open reading frame of *Danio rerio* BiP (zebrafishBiP, Uniprot Q7SZD3) into a pTrcHis-A vector for heterologous expression in *Escherichia coli*. The open reading frame cloned excluded the N-terminal signal peptide and the highly acidic sequence of eight amino acids after the peptide signal to align expression with previously studied mammalian BiP from *Mesocricetus auratus* (golden hamster, Uniprot P07823). Following PCR amplification, enzymatic digestion, ligation, and bacterial transformation, colonies were screened via colony PCR and sequencing. One clone, B1, showed 99.73% identity with the Uniprot reference, as two missense mutations (Pro→Leu) were identified. Preliminary functional assays using the malachite green method confirmed ATPase activity of hamster BiP, paving the way to test if recombinant zfBiP is biochemically active. These results lay the foundation for comparative analyses of BiP functionality across species and its potential role in the endoplasmic reticulum proteostasis and protein disaggregation.

Título: *Clonagem Molecular e Caracterização Funcional Preliminar da Chaperona BiP de Danio rerio*

A proteína BiP (Binding immunoglobulin Protein), também conhecida como GRP78, é uma chaperona dependente de ATP localizada no retículo endoplasmático (RE) e desempenha um papel fundamental na manutenção da homeostase proteica celular. Como membro da família Hsp70, a BiP atua nos processos de enovelamento, montagem, transporte e degradação de proteínas, além de ser um componente central da resposta a proteínas mal enoveladas (UPR, *Unfolded Protein Response*). O presente estudo teve como objetivo a clonagem molecular e a caracterização funcional preliminar da BiP de Danio rerio (zfBiP), com o intuito de avaliar a sua conservação evolutiva e funcionalidade comparada a ortólogos de mamíferos. Essa abordagem baseia-se na hipótese de que as chaperonas dependentes de ATP apresentam alto grau de conservação estrutural e funcional ao longo da evolução dos vertebrados, refletindo sua importância universal na proteostase e nos mecanismos celulares de resposta ao estresse.

A sequência codificante aberta (ORF) da BiP de *Danio rerio* (Uniprot Q7SZD3) foi clonada no vetor de expressão pTrcHis-A, que contém um promotor *trc* fortemente induzido por IPTG, permitindo a expressão heteróloga em *Escherichia coli*. De forma a alinhar a expressão da BiP de peixe-zebra às condições experimentais previamente utilizadas com a BiP de hamster dourado (*Mesocricetus auratus*, Uniprot P07823), a região N-terminal correspondente ao peptídeo sinal e

à sequência adjacente altamente ácida de oito aminoácidos foi removida da ORF. Essa exclusão, justifica-se pelo fato de que o peptídeo sinal é funcional apenas em células eucarióticas e sua presença poderia comprometer a expressão e a solubilidade da proteína em sistemas bacterianos.

O processo experimental incluiu múltiplas etapas de biologia molecular: amplificação do gene por PCR a partir de cDNA, digestão dupla com enzimas de restrição NheI e BamHI, ligação do inserto ao vetor, transformação bacteriana em células competentes de *E. coli* STBL3 e triagem das colônias transformadas por PCR de colônia. A análise das colônias positivas foi seguida por purificação de plasmídeos (*mini-prep*) e sequenciação. Entre as amostras obtidas, a colônia denominada B1 apresentou a sequência mais fiel ao gene de referência, com 99,73% de identidade com a sequência depositada no banco de dados Uniprot. Foram identificadas duas mutações do tipo *missense* (Pro→Leu) nas posições 339 e 378, possivelmente resultantes de erros cometidos pela polimerase ou variantes naturais da espécie. Estas substituições podem alterar propriedades da proteína, como flexibilidade estrutural ou estabilidade térmica, e, portanto, requerem investigação futura para elucidar possíveis impactos funcionais.

Para validar o sistema experimental e os métodos de análise bioquímica, foi realizado um ensaio preliminar de atividade ATPásica utilizando a BiP de hamster como controle positivo. Esse ensaio, baseado no método colorimétrico do verde de malaquita, quantifica o fosfato inorgânico liberado durante a hidrólise de ATP. O complexo formado entre o fosfato e o corante verde de malaquita é detetado por espectrofotometria a 623 nm, sendo a intensidade da cor proporcional à atividade enzimática. Os resultados confirmaram a atividade ATPásica esperada para a BiP de hamster, demonstrando que as condições experimentais — composição do tampão, temperatura, tempo de incubação e proporção de reagentes — são adequadas e reprodutíveis. Essa validação estabelece a base para futuros testes comparativos de atividade entre a BiP de hamster e a zfBiP recombinante.

Do ponto de vista conceitual, a escolha de *Danio rerio* como organismo modelo é estratégica, pois o peixe-zebra apresenta grande conservação genética com mamíferos e é amplamente utilizado em estudos de biologia molecular, desenvolvimento e doenças neurodegenerativas. A análise funcional de chaperonas como a BiP neste modelo pode oferecer insights valiosos sobre os mecanismos de controle de qualidade proteica no RE, especialmente no contexto de doenças associadas á acumulação de proteínas mal enoveladas, como Alzheimer, Parkinson e outras patologias resultantes de “misfolding” proteico. Além disso, o estudo da BiP em *Danio rerio* contribui para compreender como processos evolutivos moldaram a versatilidade das chaperonas no restabelecimento da homeostase celular em de condições celulares adversas, como stress oxidativo e sobrecarga proteica.

A BiP exerce sua função através de um ciclo dependente de ATP, alternando entre estados conformacionais de alta e baixa afinidade pelo substrato. Na forma ligada ao ATP, a BiP adota uma conformação aberta, permitindo o rápido reconhecimento e liberação de polipeptídeos

parcialmente enovelados. Após a hidrólise de ATP em ADP, ocorre uma mudança estrutural que promove o fechamento do domínio de ligação ao substrato, estabilizando temporariamente a interação com a proteína cliente. Esse ciclo é finamente regulado por co-chaperonas da família ERdj (J-domain proteins), que estimulam a atividade ATPásica, e pelos fatores de troca de nucleotídeos (NEFs), responsáveis pela liberação de ADP e reativação da BiP. Essa dinâmica confere à BiP a capacidade de monitorarizar continuamente a conformação das proteínas recém-sintetizadas, garantindo que apenas aquelas devidamente enoveladas sejam encaminhadas para o destino correto dentro da célula.

No presente trabalho, o foco principal foi o desenvolvimento de uma base experimental robusta para a expressão e caracterização da BiP recombinante de peixe-zebra. A confirmação da clonagem correta, a validação do vetor de expressão e a implementação de ensaios de atividade enzimática são passos essenciais para análises comparativas posteriores. Pretende-se, em etapas futuras, expressar a zfBiP em larga escala, purificá-la por cromatografia de afinidade via *His-tag* e realizar ensaios funcionais detalhados, incluindo medições cinéticas de ATPase e testes de interação com proteínas modelo de agregação, como domínios J recombinantes. Esses estudos permitirão avaliar o grau de conservação funcional entre a zfBiP e suas contrapartes de mamíferos, e determinar se variações pontuais, como as mutações observadas na colônia B1, afetam a sua capacidade de catalisar a hidrólise de ATP e de prevenir agregação proteica.

Os resultados obtidos até o momento demonstram o sucesso da etapa de clonagem molecular e a viabilidade do sistema de expressão bacteriano para a produção da BiP de *Danio rerio*. Além disso, o ensaio preliminar com a BiP de hamster confirma a funcionalidade do método adotado para a análise ATPásica, constituindo um importante passo para os estudos comparativos planejados. Essa integração entre biologia molecular e bioquímica experimental representa uma abordagem abrangente para investigar as propriedades de chaperonas endoplasmáticas num contexto evolutivo.

Conclui-se que o presente trabalho estabelece as bases necessárias para futuras análises estruturais e funcionais da BiP de *Danio rerio*. A alta identidade com a sequência de referência e a integridade do gene clonado confirmam a eficiência do protocolo de clonagem. A metodologia padronizada poderá ser aplicada a outras chaperonas do retículo endoplasmático, como a Grp94, ampliando a compreensão dos mecanismos de homeostase proteica nos vertebrados. Num contexto mais amplo, a caracterização comparativa dessas proteínas pode fornecer insights relevantes para o desenvolvimento de terapias baseadas em chaperonas, com potencial de modular a resposta ao stress do retículo e restaurar o equilíbrio proteico em condições patológicas.

Assim, o estudo da BiP de *Danio rerio* reforça a importância das chaperonas dependentes de ATP como pilares da estabilidade proteica celular e da defesa contra o stress proteotóxico. Os resultados obtidos nesta etapa preliminar, embora introdutórios, representam um avanço

significativo na consolidação de um modelo experimental que permitirá explorar, em detalhe, a funcionalidade, a conservação evolutiva e o potencial terapêutico das chaperonas do retículo endoplasmático.

Table of contents

1. Introduction

The study of ATPase-dependent chaperones BiP and Hsp70 in zebrafish may provide a rich context for understanding the intricate roles these proteins play in cellular homeostasis. This introduction outlines not only the fundamental aspects of these chaperones but also their roles in cell proteostasis and implications in neurodegenerative diseases associated with protein aggregation. By focusing on zebrafish as a model organism, this research seeks to enhance our understanding of chaperone proteins in various cellular functions and their connection to neurodegenerative diseases.

Heat shock proteins (HSPs), including Hsp90 and Hsp70, are a class of proteins that play crucial roles in protein folding, assembly, and degradation, thus preventing cellular dysfunction (Audouard et al., 2011) (Griffith & Holmes, 2019). HSPs such as Hsp90 and Hsp70 are essential for the folding and assembly of various cellular proteins; they also regulate the kinetics of partitioning between folding, translocation, and aggregation within the cell (Roberts et al., 2010). Building on this framework, this chapter will also focus on the contributions of protein aggregation to neurodegeneration. The pathological accumulation of misfolded proteins is not merely a bystander effect; rather, it plays a central role in the mechanism of neuronal dysfunction and cell death (Maziuk et al., 2017). We will explore how aggregation-prone proteins initiate and propagate cellular damage, emphasizing the role of chaperones in mitigating these processes.

Chaperones and co-chaperones play a crucial role in preventing protein aggregation, particularly under stress conditions, and imbalances in their levels have been linked to protein misfolding in neurons (Bohush et al., 2019). These highly conserved molecular chaperones are present in all living cells and participate in key processes associated with development, differentiation, aging, and death (Sottile & Nadin, 2017). Aggregated proteins disrupt cellular processes and foster neuroinflammation, thus exacerbating the neurodegenerative process (Sottile & Nadin, 2017). This critical connection between protein aggregation and disease pathology will be established through a synthesis of current research findings.

A deep understanding of protein homeostasis is essential for examining the roles of molecular chaperones, which are vital in mitigating the detrimental effects of misfolded proteins (Bross et al., 1999). In this chapter, we will discuss the various chaperone systems, focusing on their functions in maintaining cellular protein integrity. The Hsp70 cytoplasmic system and the BiP endoplasmic reticulum (ER) system represent two key players in this context. We will analyze how these systems interact with misfolded proteins and the implications for cellular health, presenting an overview of the importance of molecular chaperones in neurodegenerative diseases.

The following topic will highlight the specific functions of Hsp70 and BiP chaperones, detailing their contributions to protein folding and disaggregation processes. Through a nuanced examination of these chaperones, we will describe how they can restore protein homeostasis and prevent the toxic accumulation of misfolded proteins (Sottile & Nadin, 2017). This analysis will provide insight into the therapeutic potential of targeting these molecular chaperones in the context of neurodegenerative diseases.

As we proceed to address current gaps in our understanding of the therapeutic potential of targeting molecular chaperones, the penultimate topic will evaluate existing research, clarifying areas where further investigation is necessary. We will consider how insights gained from studying molecular chaperones can provide a pathway for innovative therapeutic strategies aimed at combating the progression of neurodegenerative diseases.

1.1 Overview of Neurodegenerative Diseases

Neurodegenerative diseases are a group of disorders characterized by progressive degeneration of the structure and function of the nervous system (Zhou et al., 2022). These diseases pose significant challenges not only for those affected but also for caregivers and healthcare systems. The hallmark of many neurodegenerative diseases is the accumulation of misfolded proteins, leading to toxic aggregates that disrupt cellular function and induce neurodegeneration (Nakamura & Lipton, 2010). Understanding these diseases requires a thorough examination of their classifications, clinical manifestations, and molecular mechanisms.

Neurodegenerative diseases can be primarily classified based on the specific proteins involved in aggregation. This classification leads to the identification of several major groups, including tauopathies and synucleinopathies. Tauopathies are characterized by the abnormal accumulation of tau protein, predominantly affecting neurons and leading to cellular dysfunction (Guo et al., 2017). Synucleinopathies, on the other hand, are marked by the aggregation of alpha-synuclein, primarily affecting dopaminergic neurons, as observed in conditions like Parkinson's disease (Zampar et al., 2024). Other groups include polyglutamine diseases, which are caused by CAG (coding for glutamine) repeat expansions, with Huntington's disease being the most recognized representative (Perri et al., 2016). Each group exhibits unique pathophysiological features, linked not only to the nature of the protein aggregates but also to the neuronal populations involved (Lee et al., 2010).

Clinical manifestations of neurodegenerative diseases vary substantially, reflecting the specific neuronal circuits implicated in each disorder. For instance, patients with Alzheimer's disease often present with memory deficits, language difficulties, and disorientation due to the neurodegeneration primarily affecting the hippocampus and cortex (Ullman, 2013). Conversely, Parkinson's disease is characterized by movement disorders, such as tremors, rigidity, and bradykinesia, resulting from the loss of dopaminergic neurons in the substantia nigra (Galván & Wichmann, 2008). This variability highlights the importance of understanding the underlying neuronal target areas and the associated clinical presentations to better approach diagnosis and treatment.

At the molecular level, common mechanisms of neurodegeneration often involve protein misfolding, oxidative stress, mitochondrial dysfunction, and neuroinflammation (Jellinger, 2010). The misfolded proteins not only disrupt normal cellular function but also engage the proteostasis network, leading to impaired protein quality control (Jellinger, 2010). This impairment can activate stress responses such as the unfolded protein response (UPR), autophagy, and the heat shock response, further complicating the cellular environment and exacerbating neurodegeneration (Lackie et al., 2017). The study of these molecular mechanisms sheds light on potential therapeutic strategies that could target shared pathways across multiple neurodegenerative diseases.

Genetic factors play a pivotal role in susceptibility to neurodegenerative diseases associated with protein aggregation (Ruffini et al., 2020). Numerous genes have been implicated, such as APP, PSEN1, and PSEN2 in Alzheimer's disease, and SNCA in Parkinson's disease (Perri et al., 2016). These genetic factors can influence not only the risk of developing the disease but also the age of onset and disease progression (Imbimbo et al., 2005). As research progresses, the identification of mutations and polymorphisms associated with these diseases has facilitated the development of animal models to study disease mechanisms and test potential therapeutic interventions (Ormandy et al., 2011). These genetic insights are crucial for advancing precision medicine approaches that could tailor treatments based on an individual's genetic makeup, opening new avenues for more effective disease management (Galbreath et al., 2013).

The convergence of genetic insights with cellular and molecular biology contributes to a more comprehensive understanding of neurodegenerative diseases (Mathur & Sutton, 2017). Potential strategies include small molecules that promote proper folding, immunotherapies targeting aggregated species, and modulators that enhance the efficacy of the proteostasis network (Wareham et al., 2022). The ongoing exploration of these avenues underscores the urgency of finding effective treatments for neurodegenerative diseases, which currently impose a heavy burden on individuals and healthcare systems worldwide.

In conclusion, the comprehensive understanding of neurodegenerative diseases necessitates a multi-faceted approach encompassing their classifications, clinical presentations, and underlying molecular mechanisms. With advancements in genetic research and therapeutic development, there is hope for improved outcomes for individuals afflicted by these devastating conditions. The intricate interplay between protein aggregation and neurodegeneration remains a critical area of study, promising new avenues for exploration and intervention in the pursuit of effective treatments.

1.2 Mechanisms of Protein Aggregation

The mechanisms of protein aggregation are central to understanding neurodegenerative diseases. These diseases are characterized by the misfolding of proteins, which subsequently leads to their aggregation into structures such as amyloid plaques and neurofibrillary tangles (Soto & Satani,

2010). The biochemical pathways involved in protein misfolding are multi-faceted and often begin with intrinsic protein instability, environmental stressors, or alterations in the cellular landscape (Nakamura & Lipton, 2010). Proteins that misfold in the cellular environment can trigger various stress responses, contributing to a domino effect of cellular dysfunction (Nakamura & Lipton, 2010).

Post-translational modifications (PTMs) significantly influence the chances of proteins to aggregate (Schaffert & Carter, 2020). These modifications include phosphorylation, ubiquitination, and glycosylation, all of which can affect protein folding and stability (Schaffert & Carter, 2020). PTMs can alter protein properties, such as solubility and conformational flexibility, thus impacting the likelihood of aggregation (Schaffert & Carter, 2020). For instance, phosphorylation of tau protein is known to promote its aggregation into neurofibrillary tangles, characteristic of Alzheimer's disease (Sierra-Fonseca & Gosselink, 2018).

Molecular chaperones play a vital role in maintaining protein homeostasis by assisting in proper folding and preventing aggregation (Nakamura & Lipton, 2010). Hsp70 and Hsp90, for example, are known to recognize misfolded proteins and facilitate their refolding or target them for degradation via the proteasome (Yamamoto et al., 2014). This process is crucial for cellular health, as it prevents the accumulation of toxic protein aggregates. The presence of molecular chaperones can stabilize nascent polypeptides, thus preventing them from adopting aggregating conformations (Johnston et al., 1998).

The cellular environment significantly affects protein stability and aggregation. Factors such as pH, temperature, and ionic strength can influence protein conformation and interactions (Ortbauer, 2013). In conditions where the cellular environment becomes disrupted, proteins may begin to aggregate due to changes in solubility and stability (Ortbauer, 2013). For instance, acidic conditions can promote the aggregation of amyloid-beta peptide, a key player in Alzheimer's pathology (Lee et al., 2020). Similarly, elevated temperatures can lead to thermal denaturation, a common trigger for protein misfolding and aggregation.

The size and structure of protein aggregates are also critical in determining their toxicity to

neurons (Lee et al., 2020). Smaller aggregates, often referred to as oligomers, may be more toxic than larger fibrillar structures due to their increased ability to interact with cellular membranes and disrupt cellular signaling pathways (Maziuk et al., 2017). This is especially relevant in Alzheimer's disease, where soluble oligomers of amyloid-beta are believed to interfere with synaptic function and contribute to a cognitive decline (Bulic et al., 2011). Understanding the dynamics between aggregate size, structure, and neurotoxicity can provide insights into the underlying mechanisms of neurodegeneration.

Genetic mutations can significantly influence the aggregation process of specific proteins implicated in neurodegenerative diseases (Nakamura & Lipton, 2010). For instance, mutations in the gene encoding alpha-synuclein lead to familial forms of Parkinson's disease, resulting in the formation of aggregates that disrupt neuronal function (Wang, 2005). Such mutations can introduce conformational changes that predispose the protein to misfolding, thus altering its aggregation propensity (Wang, 2005). This highlights the importance of genetic background in the susceptibility to neurodegenerative disorders associated with protein aggregation.

To combat the accumulation of protein aggregates, cells employ various mechanisms to restore proteostasis (Ciechanover & Kwon, 2017). Autophagy and the ubiquitin-proteasome system are two main pathways that facilitate the degradation of misfolded proteins (Ciechanover & Kwon, 2017). Autophagy can engulf large aggregates and degraded organelles, allowing for cellular repair and renewal (Ciechanover & Kwon, 2017). The ubiquitin-proteasome pathway involves tagging damaged proteins for destruction, but can become overwhelmed in neurodegenerative states (Li et al., 2022). Understanding how cells maintain proteostasis helps elucidate the challenges that arise when these systems are compromised in diseases characterized by protein aggregation.

Extracellular factors also play a significant role in protein aggregation dynamics. For example, the presence of amyloid-beta in the brain can catalyze the aggregation of soluble proteins and enhance their toxic effects (Bigi et al., 2023). The interactions between amyloid-beta and other proteins create a complex environment that accelerates disease progression (Morris et al., 2008). In summary, the mechanisms underlying protein aggregation in neurodegenerative diseases

involve a complex interplay of biochemical pathways, post-translational modifications, molecular chaperones, and the cellular environment. Understanding these mechanisms is crucial for identifying therapeutic targets aimed at mitigating the progression of these debilitating conditions. By exploring the multifaceted nature of protein aggregation, researchers can develop strategies to enhance cellular resilience and potentially halt the advance of neurodegenerative diseases rooted in misfolded proteins.

1.3 Background on Chaperones

ATPase-dependent chaperones, particularly BiP and Grp94, are integral components of the cellular machinery, facilitating the proper folding of proteins and maintaining cellular homeostasis (Kim et al., 2013). The distinct structural features that characterize ATPase-dependent chaperones set them apart from non-chaperone proteins. These features include the presence of ATP-binding domains and substrate-binding domains, allowing them to assist in protein folding dynamically and effectively.

BiP and Grp94, members of the Hsp70 and Hsp90 families, both illustrate the importance of chaperone interactions with the client proteins. "The interactions between BiP and Grp94 with their client proteins underscore the importance of chaperones in cellular environments, facilitating proper protein folding and preventing aggregation" (Marzec et al., 2011). The ATPase activity integral to these chaperones facilitates binding and releasing client proteins, enabling them to fold correctly. This cycle is essential for various cellular pathways, including secretion, protein turnover, and stress responses, where the demand for effective protein handling is particularly high (Saibil, 2013).

Research involving zebrafish as a model organism has revealed unique evolutionary adaptations in chaperone function compared to their mammalian counterparts. Zebrafish exhibit unique genetic and physiological characteristics that significantly enhance the study of chaperone function, enabling researchers to investigate fundamental biological processes in a living organism (Bellipanni et al., 2016). Additionally, the evolutionary conservation of BiP and Grp94 across species allows for effective comparative studies that shed light on the adaptability and fine-tuning of chaperone function in response to different cellular environments.

When exploring the methodologies involved in studying BiP and Grp94, molecular cloning is one of the most efficient techniques. Cloning facilitates the gene expression of these chaperones, providing insight into their structural and functional properties. However, challenges can often arise during the cloning process, including challenges related to vector selection and insert orientation. Identifying optimal conditions and strategies can help with these challenges, ensuring successful cloning results. For instance, the optimization of bacterial transformation can dramatically influence recombinant protein expression levels, with successful techniques leading to higher yields of purified proteins essential for the functional assessments. This efficiency is a priority, as the recovery of high quantities of chaperone proteins directly impacts downstream analyses.

The purification of these chaperones, particularly through affinity chromatography, requires meticulous optimization to obtain high-purity samples. Factors such as buffer composition, binding conditions, and elution strategies must be carefully considered to maximize yield and purity. High-quality purified proteins are critical for accurate functional assays, enabling researchers to dissect the mechanisms by which BiP and Grp94 facilitate proper protein folding and function within the cellular environment. Understanding how these chaperones operate at a biochemical level also paves the way for broader investigations into their roles in various physiological and pathological contexts.

Biochemical assays are used to characterize the functionality of BiP and Grp94, with ATPase activity assays being among the most informative. These assays allow researchers to
observe the energy dynamics that underlie chaperone activity, further elucidating the molecular mechanisms involved in protein folding. By evaluating the functional properties of these chaperones using various biochemical analyses, researchers can gain insights into not only their roles within the cell but also the consequences of their malfunction, which can lead to diseases such as neurodegeneration and cancer.

The study of chaperones in zebrafish presents an avenue for expanding our understanding of protein folding at a broader biological level. By integrating findings from zebrafish models,

researchers can contribute to a more comprehensive understanding of the molecular interactions that govern protein destiny under various stress conditions. Through these multifaceted studies, the intricate tapestry of chaperone biology unfolds, revealing the elegance and complexity of cellular protein management.

1.4 Importance of ATPase-Dependent Chaperones

ATPase-dependent chaperones are integral to maintaining protein homeostasis within the cell, particularly under conditions that induce stress or misfolding. As mentioned, these specialized proteins play crucial roles in the folding, assembly, and degradation of polypeptides, ensuring that proteins achieve their functional forms (Pobre et al., 2018). The significance of these chaperones extends beyond mere protein folding; they are central to cellular health, actively preventing aggregate formation and supporting proper protein transport through various biological pathways (Hiller & Burmann, 2018). In this topic, we will explore the functional mechanisms of BiP and Grp94, their evolutionary significance, and the challenges faced during their characterization, particularly within the context of zebrafish as a model organism.

BiP, a member of the Hsp70 family, interacts with unfolded proteins through its ATPase activity, resulting in a cycle where substrates are sequentially bound and released as shown in Figure 1.1 (Wang et al., 2017). The ATP binding and hydrolysis cycle is crucial, as it drives conformational changes in the chaperone, allowing it to assist client proteins in reaching their native states (Maharaj et al., 2016). Similarly, Grp94, an Hsp90 family member, also employs its ATPase activity to regulate its interactions with client proteins. The coordination of ATP hydrolysis and client protein release is vital for the efficient functioning of these chaperones in a cellular environment (Maharaj et al., 2016).

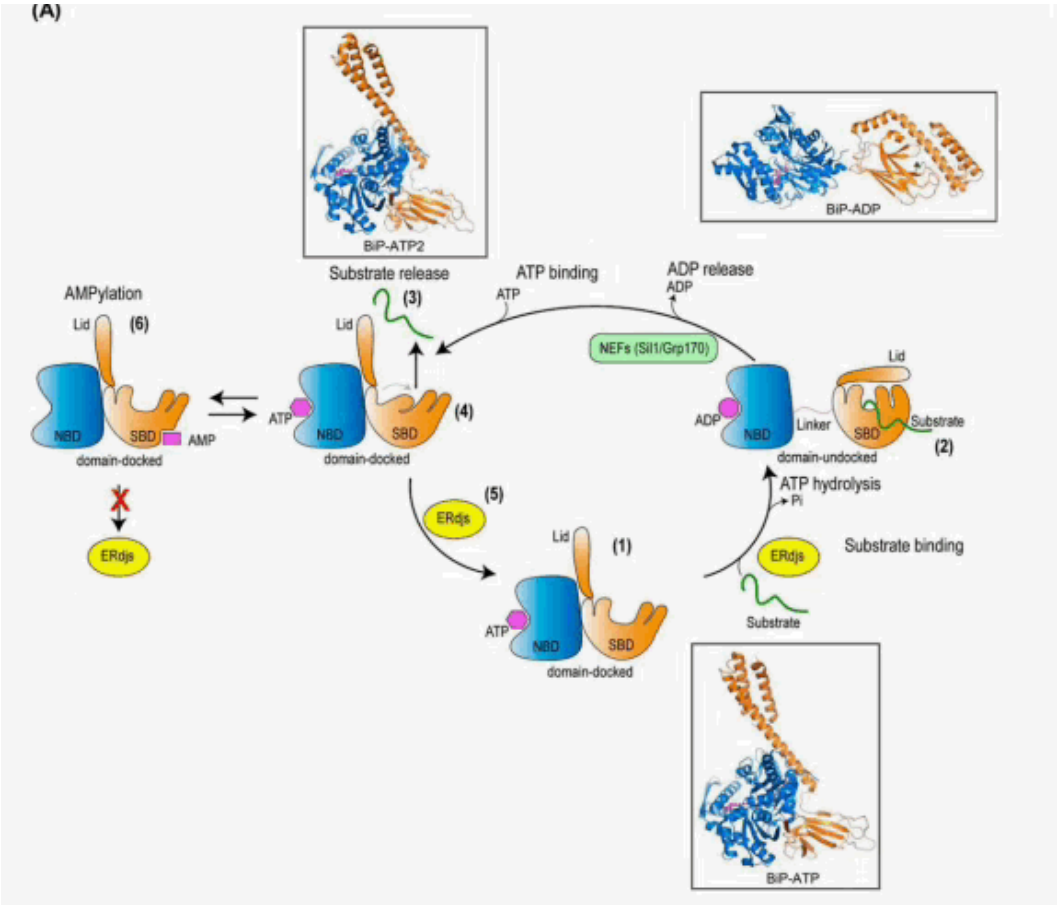

Figure 1.1 BiP ATPase Cycle: This schematic depicts the conformational changes of BiP during its ATPase cycle. In the ATP-bound form, the NBD (blue) and SBD (orange) are docked with an open lid, resulting in high substrate binding but rapid release. ATP hydrolysis causes undocking of these domains and lid closure, increasing substrate affinity but slowing binding and release. The cycle is regulated by ERdjs, which interact with unfolded proteins and promote ATP hydrolysis. Substrate release is facilitated by NEFs, and ATP binding induces a conformational change that expels the substrate. Interaction with ERdjs repositions the binding pocket for another cycle. AMPylation inactivates BiP, locking it into a "domain-docked" state, preventing ERdj interaction. Insets show structural states: open ATP-bound (PDB 5e84), ADP-bound NBD (PDB 5evz), SBD (PDB 5e85), and closed ATP-bound (PDB 6asy). (Faye et al., 2019)

A critical area of investigation involves the structural features of ATPase-dependent chaperones, which facilitate their interactions with substrate proteins. Each chaperone contains distinct domains that are essential for its ATPase and substrate- binding functions. For instance, BiP is characterized by an N-terminal ATPase domain and a C-terminal substrate-binding domain. These structural elements enable BiP to perform its dual role of folding assistance and quality

control. The conformation shifts driven by ATP hydrolysis in these chaperones allow for a dynamic interaction with various polypeptides (Wang et al., 2017). An in-depth understanding of these structures enhances our comprehension of the molecular underpinnings of protein folding.

Moreover, the study of ATPase-dependent chaperones in zebrafish offers vital contributions to understanding cellular processes, particularly under stress conditions. As these fish can withstand various environmental stresses, they serve as an ideal model for investigating the chaperone response in vivo (Krone et al., 2003). Insights gained from these studies may also inform broader applications in human health, especially concerning diseases related to protein misfolding. Understanding the mechanisms through which BiP and Grp94 promote cellular resilience against stress opens avenues for developing therapeutic strategies aimed at enhancing chaperone activity.

The implications of research into ATPase-dependent chaperones are vast, stretching from fundamental biology to potential clinical applications. The refinement of experimental methodologies aimed at studying these proteins will give valuable insights into their roles not only in normal physiological processes but also in disease states. Their critical roles in protein folding, structural maintenance, and cellular stress responses highlight their significance in maintaining protein homeostasis. As this field evolves, the relationship between chaperones and cellular health will become clearer, emphasizing the need for continued investigation into these essential proteins.

1.5 Hsp70 Cytoplasmic System: Function and Mechanism

At the molecular level, Hsp70 functions through a sophisticated mechanism that involves recognizing and binding to misfolded proteins. The specificity of Hsp70 is primarily directed by the exposure of hydrophobic residues that are typically hidden in correctly folded proteins. When misfolding occurs, these hydrophobic regions become exposed, triggering Hsp70's binding action. This double-edged sword of misfolded proteins, which presents a potential danger to cellular integrity, becomes a target for Hsp70's protective function. Once bound, Hsp70 stabilizes these proteins, preventing further aggregation and enabling them to refold properly under suitable conditions (Mayer and Bukau, 2005).

A crucial aspect of Hsp70's mechanism is its relationship with ATP hydrolysis. The cycle of ATP binding and hydrolysis is essential for Hsp70's function as shown in Figure 1.1 for BiP, the Hsp70 resident in the ER. The subsequent hydrolysis of ATP to ADP leads to a tighter binding state, effectively locking the substrate in place. This ATP-driven cycle not only facilitates the proper folding of proteins but also plays a significant role in preventing aggregation by promoting the release of properly folded proteins back into the cellular environment (Rios & Barducci, 2014). Thus, the dynamic interplay between ATP binding and hydrolysis is integral to Hsp70's chaperoning activity.

Under conditions of cellular stress, such as heat shock or oxidative stress, proteins may form aggregates that were previously folded correctly. Hsp70 is equipped with the ability to disaggregate these pre-formed structures (Wentink et al., 2020). During stress conditions, Hsp70 can cooperate with other co-chaperones like Hsp40, recruiting them to facilitate the disaggregation process. This collaboration improves the ability of the cellular chaperoning network to tackle protein aggregates more efficiently (Nogueira et al., 2018).

Moreover, Hsp70 interacts with the cellular ubiquitin-proteasome system (UPS) to orchestrate an effective response to damaged proteins. While Hsp70 assists in refolding misfolded proteins, it also identifies irreparably damaged substrates. Such substrates are polyubiquitinated, a tagging process that signals them for degradation by the proteasome (Moran et al., 2009). This dual role of Hsp70 in both repair and removal of damaged proteins underscores its significance in maintaining proteostasis and preventing the detrimental accumulation of toxic aggregates that could lead to cellular dysfunction.

The therapeutic potential of enhancing Hsp70 activity in the context of neurodegenerative diseases has garnered increasing interest. Research has demonstrated that upregulating Hsp70 in cellular models can alleviate the toxic effects of misfolded proteins, highlighting the chaperone's potential as a target for therapeutic intervention. For instance, in models of Alzheimer's disease, increasing the levels of Hsp70 have been associated with reduced amyloid-beta aggregates, suggesting that bolstering Hsp70 might serve as a viable strategy to combat neurodegenerative pathology (Hoshino et al., 2011).

Post-translational modifications (PTMs) are critical not only for regulating Hsp70 activity but also, for influencing its interactions with client proteins. Modifications such as phosphorylation and ubiquitination can alter the binding affinity of Hsp70 and impact its chaperoning efficiency (Lackie et al., 2017). These regulatory mechanisms are an area of ongoing research, demonstrating the complexity of Hsp70's functions and underscoring the need to understand how these molecular regulations can be harnessed for therapeutic benefit in neurodegenerative diseases. Moreover, the specific interactions Hsp70 has with neuronal proteins suggest that enhancing its function could directly improve cellular health and promote resilience against neurodegenerative decline (Lu et al., 2014).

Investigating the specific interactions of Hsp70 with neuronal proteins is essential for understanding its role in neurological health. Hsp70 associates with several neuronal proteins and has been implicated in processes linked to synaptic plasticity and stress responses. For example, Hsp70's interaction with proteins involved in neurotransmission and synaptic function suggests a protective role that extends beyond simple protein folding (Turturici et al., 2011). Understanding how these interactions contribute to neuronal health could reveal critical insights into the mechanisms underlying neurodegenerative diseases.

In conclusion, the Hsp70 cytoplasmic chaperone system is integral to maintaining protein homeostasis in the face of misfolding and aggregation. Its ability to recognize, bind, and refold misfolded proteins highlights its importance, particularly in neurodegenerative diseases characterized by protein misfolding. The interplay between ATP hydrolysis, interaction with the ubiquitin-proteasome system, and regulatory mechanisms through post-translational modifications illustrates the multifaceted nature of Hsp70. The relationship between Hsp70 and neuronal proteins further emphasizes that understanding these interactions is essential for developing new approaches to enhance neuronal resilience against aggregated proteins.

1.6 BiP Endoplasmic Reticulum System: Function and Mechanism

The BiP (Binding immunoglobulin Protein) ER system is a critical component of the cellular machinery responsible for maintaining protein homeostasis. At its core, BiP serves as a molecular chaperone, predominantly localized within the ER, and plays an essential role in the

folding, assembly, and quality control of nascent proteins entering the secretory pathway. BiP operates primarily through a cycle of binding and release, utilizing the energy derived from ATP hydrolysis to facilitate proper protein folding (Figure 1.1). This process begins when newly synthesized polypeptides enter the ER lumen, where BiP recognizes and binds to exposed hydrophobic residues that signal misfolding. By stabilizing these nascent proteins, BiP prevents premature aggregation, ensuring that only properly folded proteins are allowed to progress through the secretory pathway (Jin et al., 2017; Pobre et al., 2018).

The binding of BiP to misfolded proteins initiates a cascade of chaperoning activities, including attempts at refolding, that are essential for maintaining cellular integrity. In instances where proteins cannot achieve their correct conformation, BiP participates in the ER-associated degradation (ERAD) pathway (Wang et al., 2017). This process is an essential mechanism for handling persistent misfolded proteins. The role of BiP in this context underscores its significance in cellular quality control systems, as accumulation of misfolded proteins can lead to ER stress and activation of the unfolded protein response (UPR) (Pobre et al., 2018).

BiP's interactions with other molecular chaperones and co-chaperones in the ER are also critical for its function. This network of chaperones integrates several quality control pathways, creating a robust defense against proteotoxic stress. For example, BiP collaborates with nucleotide exchange factors (NEFs) and co-chaperones (ERdjs) that facilitate its activity and regulate the chaperoning cycle. This multifaceted interaction landscape enhances BiP's ability to respond to misfolded proteins effectively, enabling a coordinated effort in protein folding and degradation (Behnke et al., 2015). Furthermore, post-translational modifications (PTMs) of BiP significantly influence its chaperoning efficiency and effectiveness. Modifications such as phosphorylation and glycosylation can alter BiP's conformation and binding affinity, thus impacting its interaction with client proteins (Wang et al., 2017). This regulatory framework allows the ER to adapt to various stressors, ensuring that BiP remains efficient in its role as a chaperone.

In therapeutic contexts, targeting the BiP ER system presents a promising avenue for addressing neurodegenerative diseases (Gorbatyuk & Gorbatyuk, 2013). Strategies

aimed at enhancing BiP function or upregulating its expression could improve the degradation of toxic protein aggregates and restore cellular homeostasis. Modulating the activity of BiP, whether through pharmacological agents or genetic approaches, has shown potential in preclinical models, highlighting the therapeutic promise of harnessing this chaperoning system (Wang et al., 2017).

In summary, the BiP ER system is integral to maintaining protein homeostasis in the face of the continual challenges posed by misfolded proteins. By facilitating correct protein folding, engaging in quality control processes, and collaborating with other chaperones and degradation systems, BiP plays an essential role in ensuring cellular health. Its significance is further amplified in the context of neurodegenerative diseases, where maintaining the functionality of this chaperoning system could hold therapeutic potential for combating protein aggregation-related pathologies. Continued exploration into the mechanisms and functions of BiP may lead to innovative strategies aimed at restoring balance within the cellular environment, ultimately benefiting individuals afflicted by neurodegeneration.

2. Materials and Methods

2.1 Materials

2.1.1 Reagents and Solutions

- **General Reagents**: Water (Milli-Q), dNTPs NZYMix (NZYtech), restriction enzymes: *Fast Digest NheI* (Thermo Scientific FD0973) and *Fast Digest BamHI* (Thermo Scientific FD0054), T4 DNA Ligase (Thermo Scientific EL0014), T4 DNA Buffer (Thermo Scientific) specific primers, DNA Polymerase (*Supreme NZYProof* MB28301), 10X Fast Digest Green Buffer (Thermo Scientific), 5X Reaction Buffer (NZYtech) and Ampicillin.
- **Specific Reagents**: ATP stock solution, BiP protein, Malachite Green, HK buffer: 50 mM HEPES, 150 mM NaCl, pH 7.4 (adjusted with KOH), HT JD protein (135 μM stock solution), and Aggregated HT JD (50 μM, heated at 53°C for 25 min).
- **Growth Media**: LB (Luria-Bertani) broth, LB agar plates supplemented with antibiotic (Ampicillin) and 70% Glycerol.
- **Kits Used**: NZYTech Kit for DNA purification (NZYGelpure MB011102) and NZYTech Kit for MiniPrep (NZYMiniprep MB01002)

2.1.2 Bacterial Strains

- *E. coli* BL21(DE3)
- *E. coli* STBL3

2.1.3 Plasmids

- hPDI(18-508)pTrcHis-A

2.1.4 Primers

- FW_: 5’ AAA TTA GCT AGC GTT GGG ACA GTG ATT GGG 3’
- RV_: 5’ ATA TAT GGA TCC CTA CAG CTC GTC CTT CTC TTC 3’

2.1.5 Equipment and Software

- Thermocycler for PCR.
- NanoDrop Spectrophotometer for DNA concentration measurement.
- Agarose gel electrophoresis system.
- Centrifuges for protein purification.
- Incubators at 30°C and 37°C.

2.2 Methods

2.2.1 Preparation of Competent Cells

1. *Escherichia coli* cultures were initially grown on an LB agar plate, from which a single colony was selected and inoculated into 5 mL of LB medium. The culture was incubated overnight at 37°C with shaking.
2. The following day, a fresh LB medium was prepared by dissolving 6.25 g of LB broth in 250 mL of distilled water, followed by sterilization via autoclaving. Once cooled, 1 mL of the overnight *E. coli* culture was inoculated into the freshly prepared medium and incubated overnight at 18°C with shaking.
3. The next morning, the optical density (OD) at 600nm of the culture was measured by diluting 100 µL of the bacterial culture in 900 µL of distilled water and analyzing the sample using a spectrophotometer. The culture was allowed to grow until an OD_{600} of approximately 0.4–0.5 was reached.
4. Once the desired OD was obtained, the culture flask was placed on ice for 10 minutes to reduce metabolic activity. The culture was then distributed into five 50-mL Falcon tubes, with 50 mL of bacterial suspension per tube. The tubes were centrifuged at 4°C for 10 minutes at 2,500 × g. The supernatant was carefully discarded, and the bacterial pellets were resuspended in 16 mL of ice-cold HK buffer. The suspension was incubated on ice for 10 minutes.
5. A second centrifugation was performed at 4°C for 10 minutes at 2,500 × g, after which the supernatant was discarded. The bacterial pellet from one tube was resuspended in 5 mL of ice-cold HK buffer and sequentially transferred to the next tube, repeating the

resuspension process until all pellets were combined into a single tube. The final suspension was incubated on ice for 10 minutes.

6. The cells were then treated with 350 µL of $CaCl_2$ (60 mM) and incubated on ice for an additional 10 minutes.
7. Finally, aliquots of 100 µL of the competent cell suspension were transferred into sterile Eppendorf tubes, flash-frozen in liquid nitrogen, and stored at -80°C until further use.

2.2.2 Backbone Preparation for Cloning

Figure 2.1 presents a vector map of the hPDI(18-508)pTrcHis-A UK233 plasmid, which harbors the open reading frame (ORF) of human protein disulfide isomerase (PDI) cloned between the *NheI* (449 bp) and *BamHI* (1931 bp) restriction sites. This plasmid was previously used to express recombinant hPDI in *E. coli*. The ampicillin resistance gene (AmpR) ensures selective pressure for maintaining the plasmid in bacterial cultures.

For the purposes of this study, the PDI ORF was removed by digesting the vector with *NheI* and *BamHI* and later replaced with the zebrafish BiP ORF, encoding the ATPase-dependent chaperone from the ER. The sequence coding for the His-tag placed upstream the *NheI* restriction site, facilitates protein purification via affinity chromatography, a critical step for characterizing the chaperone's biochemical properties. Expression of the recombinant protein is driven by the strong *E. coli* trc promoter and Lac operon, an IPTG-inducible system that ensures high-yield expression in bacterial hosts.

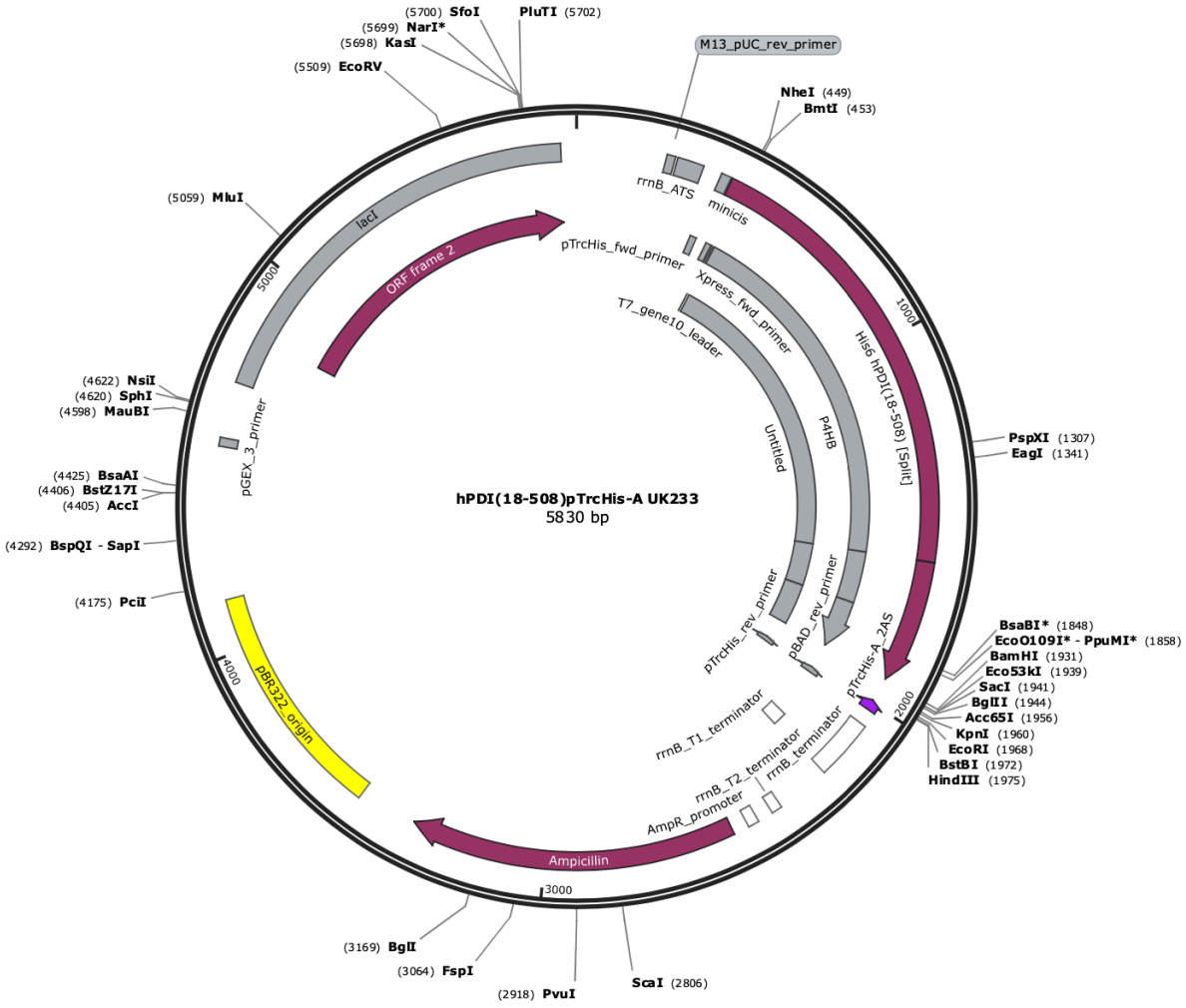

Figure 2.1: ***Plasmid Map of hpDDL(18-508)pTchis-A UK233*** This figure presents a circular map of the plasmid construct *hpDDL(18-508)pTchis-A UK233,* approximately 5,830 base pairs in length. The map illustrates the arrangement of various genetic elements, restriction enzyme sites, and functional regions within the plasmid. Notable features include multiple restriction sites *(e.g., NheI, BamHI, BsrBI, BclI, BglII, HindIII),* which facilitate cloning and molecular analysis. The different colored segments represent specific functional regions, such as promoters, genes, or selectable markers, providing a visual overview of the plasmid's structure. This map serves as a valuable reference for understanding the genetic composition of the construct, guiding subsequent cloning, sequencing, or functional experiments.

To prepare the digestion reaction, the following components were combined in a sterile microcentrifuge tube:

- 5 µL of nuclease-free water
- 2 µL of 10× Fast Digest Green Buffer
- 11 µL of plasmid DNA (232 ng/µL + 50 ng/µL) (33.2 nM)
- 1 µL of Fast Digest *NheI* (10 U)
- 1 µL of Fast Digest *BamHI* (10 U)

The reaction mixture was gently mixed and briefly spun down in a bench centrifuge. The tube was then incubated at 37°C for 15 minutes to allow complete enzymatic digestion.

Following digestion, the incubator was set to 80°C. Meanwhile, the reaction tube was placed on ice while the incubator preheated. The sample was subsequently incubated at 80°C for 5 minutes to inactivate the restriction enzymes.

An agarose gel was prepared for electrophoresis, and the digested plasmid sample was loaded into one of the wells. Gel electrophoresis was performed in 1% agarose gels under standard conditions to separate the DNA fragments.

The target DNA fragment of the expected size (~4000 bp) was excised from the agarose gel and purified using the NZYTech Gel and PCR Purification Kit, following the manufacturer's instructions.

Finally, the DNA concentration was measured using a NanoDrop to confirm successful purification.

2.2.3 Insert Preparation

2.2.3.1.PCR Amplification

Polymerase chain reaction (PCR) was performed to amplify the target DNA sequence. The reaction mixture was prepared as follows:

- 32 µL of nuclease-free water

- 10 µL of 5× Reaction Buffer
- 1 µL of dNTP mix (0.2 mM each)
- 2.5 µL of Forward Primer (0.5 µM)
- 2.5 µL of Reverse Primer (0.5 µM)
- 1 µL of DNA Template (diluted 1:10 or 1:100) zfBiP ORF amplified from cDNA (~10–100 ng)
- 1 µL of Supreme DNA Polymerase (1 U)

The following conditions were tested:

1. Three replicates of a previously obtained zebrafish BiP ORF as template to be amplified using specific primers at 58°C
2. Three replicates of a previously obtained zebrafish BiP ORF as template to be amplified using specific primers at 60°C

Additionally, two negative controls were prepared by omitting the DNA polymerase and replacing it with 1 µL of nuclease-free water:

- Control 1: Without DNA polymerase at 58°C
- Control 2: Without DNA polymerase at 60°C

The samples were placed in a gradient PCR machine with the following thermal cycling parameters:

Table 1 PCR Reaction Preparation and Cycling Conditions

Step	Temperature	Duration
Initial Denaturation	96°C	4 min
Denaturation (30 cycles)	96°C	30 sec
Annealing (Gradient)	58°C and 60°C	30 sec
Extension (30 cycles)	72°C	1 min
Final Extension	72°C	10 min
Hold	4°C	∞

Following amplification, agarose gel electrophoresis was performed to confirm the presence of the DNA fragment band of the expected size (~1900 bp).

2.2.3.2. Double Digestion of Insert

Six digestion reactions were prepared, each containing the following components:

- 14.5 µL of nuclease-free water
- 2 µL of 10× Fast Digest Green Buffer
- 1.5 µL of purified PCR product (0.5 µg total DNA)
- 1 µL of Fast Digest NheI (10 U)
- 1 µL of Fast Digest *BamHI* (10 U)

The reaction mixtures were gently mixed and briefly centrifuged using a spin-down machine. Samples were incubated at 37°C for 15 minutes to ensure complete digestion.

Following digestion, the thermoblock was set to 80°C, and samples were subsequently incubated at 80°C for 5 minutes to inactivate the restriction enzymes.

Agarose gel electrophoresis was performed to separate the DNA fragments. The expected fragment size was around 1,900 bp. The target DNA fragment was excised from the gel and purified using the NZYTech Gel and PCR Purification Kit, following the manufacturer's instructions.

Finally, the DNA concentration was measured using a NanoDrop spectrophotometer.

2.2.4 Ligation and Transformation

Ligation Reaction

Ligation reactions were prepared using T4 DNA Ligase in a total volume of 20 µL per sample.

Table 2 Ligation Reaction Setup with Different Molar Ratios

Component	1:1 Molar Ratio	1:5 Molar Ratio	Control
Backbone DNA (15 ng/µL)	2 µL	2 µL	2 µL
Insert DNA (9.3 ng/µL)	3.5 µL	15.8 µL	0 µL
10× Ligase Reaction Buffer	2 µL	2 µL	2 µL
Nuclease-free Water	12.3 µL	0 µL	15.8 µL
DNA Ligase	0.2 µL	0.2 µL	0.2 µL
Final Volume	20 µL	20 µL	20 µL

The reaction tubes were incubated initially at 22°C for 30 minutes, followed by 65°C for 10 minutes to inactivate the ligase.

Bacterial Transformation

After ligation, *E. coli* STBL3 competent cells were retrieved from the -80°C freezer. A total of six transformation reactions were prepared, using different volumes of ligated DNA:

- 5 µL of ligation mix was added to three tubes containing 100 µL of competent cells
- 10 µL of ligation mix was added to another three tubes containing 100 µL of competent cells

The transformation protocol was performed as follows:

1. Heat shock transformation:
    - Samples were incubated on ice for 20 minutes.
    - Cells were subjected to a heat shock at 42°C for 30 seconds.
    - Tubes were immediately placed on ice for 5 minutes.
2. Recovery phase:
    - 600 µL of LB medium without antibiotic was added to each tube.

- Samples were incubated at 37°C for 1 hour in a thermoblock to allow recovery and expression of the antibiotic resistance gene.

3. Centrifugation and plating:
    - Cells were centrifuged at 2300 × g for 5 minutes.
    - 450 µL of supernatant was removed from each sample.
    - The remaining cell suspension was resuspended and plated on LB agar plates containing ampicillin (LB + Amp).
    - Plates were incubated overnight at 37°C.

2.2.5 Colony Screening

Colonies from the LB + Amp plates were screened by PCR to confirm the presence of the insert. A Petri dish with a 4×4 matrix drawn on the lid was prepared by randomly selecting 16 colonies from the plates and transferring them to designated positions within the matrix. This plate was left to grow overnight at 30°C incubation. Four colonies were picked using sterile plastic tips and resuspended directly in water in PCR tubes to be used as the DNA template.

PCR Reaction Preparation

Eight PCR tubes were prepared with the following reaction mix

Table 3 PCR Reaction Preparation

Component	Volume (µL)
Nuclease-free Water	13 µL
5× Reaction Buffer	4 µL
dNTPs (0.25 mM)	0.5 µL
Forward Primer (0.025 µM)	1 µL
Reverse Primer (0.025 µM)	1 µL
Supreme DNA Polymerase (1 U)	0.5 µL

Final Volume	20 μL

The PCR reaction was performed using an annealing temperature of 58°C with the following cycling conditions:

Table 4 PCR Reaction Cycling Conditions

Step	Temperature	Duration
Initial Denaturation	96°C	4 min
Denaturation (30 cycles)	96°C	30 sec
Annealing	58°C	30 sec
Extension (30 cycles)	72°C	1 min
Final Extension	72°C	10 min
Hold	4°C	∞

After PCR amplification, an agarose gel electrophoresis was performed to analyze the results.

2.2.6 Bacterial Culture and Storage

Colony Inoculation

A single bacterial colony was inoculated into LB medium supplemented with ampicillin for overnight culture. The procedure was as follows:

1. Two Falcon tubes were prepared, each containing 5 mL of LB medium.
2. 5 μL of ampicillin (100 mg/mL) was added to each tube.
3. A sterile pipette tip was used to pick a single colony from the LB + Amp plate, and the bacteria were transferred into the Falcon tubes by immersing the tip in the medium.
4. The tubes were sealed and incubated overnight at 37°C with shaking.

Glycerol Stock Preparation

To prepare long-term glycerol stocks for bacterial storage, the following steps were performed under a flame to maintain sterility:

1. Two sterile Eppendorf tubes were prepared.
2. 645 µL of the overnight bacterial culture was transferred into each Eppendorf tube.
3. 858 µL of 70% glycerol was added to each sample.
4. The tubes were mixed gently and stored at -80°C for long-term preservation.

2.2.7 ATPase Activity Assay

The method to quantify inorganic phosphate released from ATP hydrolysis was obtained in the publication by Rauch, and Gestwicki, 2014. The method is based on the formation of a complex between malachite green and inorganic phosphate.

Sample Preparation

1. Retrieve the following samples from -80°C storage:
    - ATP stock solution (500 mM)
    - BiP protein
    - HT JD protein (135 µM stock solution)
2. Prepare HT JD Stock Solution to aggregate by mixing:
    - 472 µL of HK Buffer
    - 278 µL of HT JD (135 µM stock solution)
3. Aggregate HT JD Solution (50 µM) by incubating it at 53°C for 25 minutes.

ATPase Reaction Setup

Five Eppendorf tubes were prepared with different ATP concentrations as follows:

Table 5 ATPase Activity Assay Sample Preparation

ATP Molar Concentrations	0.5 mM	2 mM	4 mM	6 mM	9 mM
HK Buffer	477.3 µL	475.4 µL	472.8 µL	470.2 µL	466.3 µL
Mg (500 mM)	13 µL	13 µL	13 µL	13 µL	13 µL
Agg HT JD (50 µM)	130 µL	130 µL	130 µL	130 µL	130 µL

BiP (112 µM)	29 µL	29 µL	29 µL	29 µL	29 µL
ATP (500 µM)	0.65 µL	2.6 µL	5.2 µL	7.8 µL	11.7 µL

Note: ATP was added last to each reaction tube.

Standard Curve Preparation

Table 6 Standard Curve Preparation for Phosphate Quantification

PO_4 (µM)	Well ID	Working Solution KH_2PO_4 (100 µM)	Water	Final Volume (µL)
0	A1	0 µL	150 µL	150 µL
5	A2	7.5 µL	142.5 µL	150 µL
10	A3	15 µL	135 µL	150 µL
15	A4	22.5 µL	127.5 µL	150 µL
20	A5	30 µL	120 µL	150 µL
25	A6	37.5 µL	112.5 µL	150 µL
30	A7	45 µL	105 µL	150 µL
40	A8	60 µL	90 µL	150 µL
50	A9	75 µL	75 µL	150 µL
60	A10	90 µL	60 µL	150 µL
70	A11	105 µL	45 µL	150 µL
80	A12	120 µL	30 µL	150 µL
90	B1	135 µL	15 µL	150 µL
100	B2	150 µL	0 µL	150 µL

Plate Preparation and Reaction Measurement

1. Prepare the assay plate by adding the following to wells:
    - 50 µL of Malachite Green Working Solution
    - 100 µL of water
    - 50 µL of sample
2. Start the timing after adding sample, to measure time passed since first sampling.
3. After 2 minutes, add 20 µL of Citrate Stock Solution (34% w/v) to each well to stop reaction.

To assess ATPase activity over time, the reaction mixtures prepared in Table 5 were incubated at room temperature for a total duration of 240 minutes. At defined time points (0, 30, 60, 120 and 240 minutes), 50 µL aliquots were withdrawn from each reaction tube. Each aliquot was immediately transferred to a separate well of a 96-well plate pre-loaded with 100 µL of distilled water and 50 µL of Malachite Green Working Solution.

This protocol was repeated for each time point and ATP concentration, ensuring that each measurement reflected the inorganic phosphate released by ATP hydrolysis at that specific time point. Importantly, new wells were used for each time point and two replicates were done. This approach enabled the construction of time-dependent phosphate release profiles for each condition.

3. Results and Discussion

3.1 Backbone Preparation

The digestion reaction was performed using Fast Digest *NheI* and *BamHI*, followed by enzyme inactivation at 80°C.

Agarose gel electrophoresis (Figure 3.1) confirmed successful double digestion, with distinct DNA bands visible under UV light. The double digested DNA band was excised and purified using the NZYTech Gel and PCR Purification Kit. The final DNA concentration measured by NanoDrop was 13.5 ng/µL, confirming purification and suitability for downstream applications.

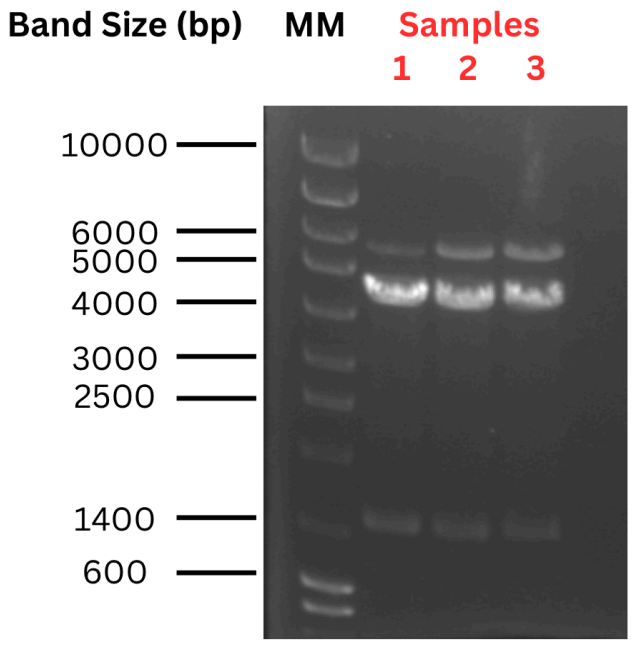

Figure 3.1: Agarose gel electrophoresis after double digestion
Around 4,351 bp
Upper Band: Single Digested DNA → 5830
Second Band: Double-digested DNA (5830 bp - 1479 → 4351)
Third Band: Insert PDI (PDI including the HisTag= 1516 bp - 37 bp → 1479*)*

3.2 Insert Preparation

The ORF of zebrafish BiP was obtained at NCBI (gene ID 378848 and NCBI Reference Sequence: NM_213058.1):

```
   1 at gcggttgctt tgcctgtttt tgctggtggc cggcagcgtg
  43 tttgccgaag aggacgataa gaaggagagt gttgggacag tgattgggat cgacctcggg
 103 accacatact cctgtgttgg agtctacaag aatggccgtg ttgagattat tgccaatgac
 163 cagggaaacc gcatcactcc gtcatacgtg gcctttacca ctgaaggaga gcggctcatc
 223 ggagatgctg cgaagaacca gctcacatcc aaccctgaaa acactgtgtt tgacgccaag
 283 aggctgatcg gacgcacatg gggcgactct tctgtgcagc aggacatcaa atacttcccc
 343 tttaaggtga tcgagaagaa aaacaagcct cacatccagc tggacatcgg ctctggtcag
 403 atgaagacgt ttgcaccgga ggaaatttcc gccatggttt tgaccaagat gaaggaaacc
 463 gcagaggctt atctgggaaa gaaggtcact catgctgtgg tcaccgttcc tgcttatttc
 523 aacgatgctc agcgtcaggc cactaaagat gctggaacca ttgctgggct gaatgtcatg
 583 aggatcatca atgagcctac ggcggctgcc attgcatacg gtctggacaa gagggacgga
 643 gagaaaaaca tcctggtgtt cgatctgggt ggtggcacct ttgacgtgtc tctgctgacc
 703 atcgataacg gcgtgtttga agtggtggcc acaaacggag acactcacct gggcggagaa
 763 gacttcgacc agcgcgtcat ggagcacttc atcaagctgt acaagaagaa gacgggcaaa
 823 gacgtgcgca aagacaaccg cgccgtgcag aagctgcgca gagaggtgga gaaggctaag
 883 agagcgctgt ctgcccagca tcaggcccgc atcgagatcg agtccttctt tgaaggagaa
 943 gatttctctg agactctcac cagagccaag tttgaggagc tcaacatgga cttgttccgc
1003 tccactatga agccggttca gaaggttctg gaggactctg acccgaagaa gccagatatc
1063 gatgagatcg tgctggtcgg cggctccact cgtatcccga agatccagca gctggtgaag
1123 gagttcttca acggaaaaga gccgtccaga ggaatcaacc ctgacgaggc cgtggcgtac
1183 ggagctgctg tccaggctgg agtcctgtcc ggagaggagg agaccggtga tctggttctt
1243 ctggacgtgt gtccgctgac tctgggcatt gagactgttg gaggagtgat gaccaaactc
1303 attcccagaa acactgttgt tcccaccaag aaatcccaga tcttctccac tgcttccgac
1363 aaccagccca ccgtcactat caaagtttat gagggcgagc gtcccctgac caaagacaac
1423 catctgctgg gcacctttga cctgacaggc atccctccag cacctcgtgg tgtcccacag
1483 atcgaggtaa ctttcgagat cgacgtcaac ggcatcctgc gcgtcaccgc cgaagacaaa
1543 ggcaccggaa acaaaaacaa gatcaccatt accaacgacc agaaccggct gacccctgag
```

1603 gacatcgaga gaatggtgaa cgaagccgag agattcgctg atgaggacaa gaaactgaag
1663 gagagaatcg acagccgcaa tgaattggag agctacgcct attccctgaa gaaccagatc
1723 ggggataaag agaaattagg cggaaagtta tcctctgaag acaaggaggc catcgagaag
1783 gcagtggagg agaagatcga gtggctggag gcgcatcagg acgccgatct ggaggaattc
1843 caggccaaaa agaaggagct ggaggaggtg gtgcagccca tcgtcagcaa actgtacggc
1903 agtgcgggag gaccaccgcc tgaagaggcc gaagagaagg acgagctgta g

The first 16 codons (48 nucleotides) code for a peptide signal that directs the newly synthesized protein to the ER in eukaryotic cells (also called secretory pathway) and therefore are useless to express the protein in *E. coli* which has no secretory pathway. The next 8 codons (24 nucleotides) code for a highly charged sequence (GluGluAspAspLysLysGluSer) that was not included as part of the golden hamster BiP previously cloned in pQE10 vector to be expressed in *E. coli* (a kind gift from David Ron, University of Cambridge). Therefore, since the main goal is to compare the zebrafish BiP with mammalian BiP from golden hamster to analyze how BiP has evolved in its chaperone function, it was decided to start the amplification at the codons gtt ggg aca..... coding for the residues ValGlyThr.

3.2.1. PCR Amplification

The PCR to amplify the ORF of zebrafish BiP starting on Val25 was carried out using specific primers and cDNA diluted 1:10 and 1:100 as a template. An agarose gel was run to check the size of the bands (Figure 3.2).

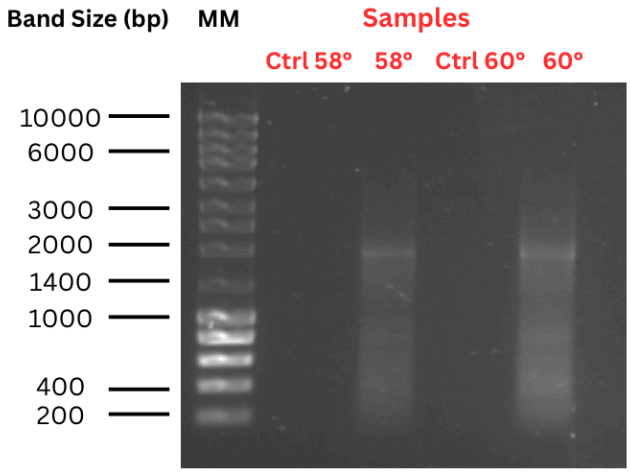

Figure 3.2: Agarose gel electrophoresis results of PCR amplifications of the zebrafish BiP open reading frame (ORF) The PCR reactions were carried out using specific primers under two annealing temperatures: 58°C and 60°C. Each reaction mixture included either new or old Supreme DNA Polymerase, with a 1:10 or 1:100 dilution of the DNA template. Negative controls lacking polymerase (Ctrl 58° and Ctrl 60°) showed no visible amplification, as expected. Amplification products were observed at both 58°C and 60°C, yielding a single band of the expected size (1882 bp), confirming successful amplification of the target sequence under both annealing conditions.

Agarose gel electrophoresis showing amplified zebrafish BiP ORF at ~1882 bp under both annealing temperatures (58°C and 60°C). Negative controls showed no amplification.

Following this, the PCR product annealed at 60°C was purified using the NZYTech PCR purification kit. The DNA concentration after purification was measured to be 178 ng/µL, confirming a sufficient yield for further experiments.

3.2.2. Double Digestion

The Clean PCR product was double digested and an agarose gel electrophoresis was run (Figure 3.3). The expected DNA band with 1882 bp was observed in the gel.

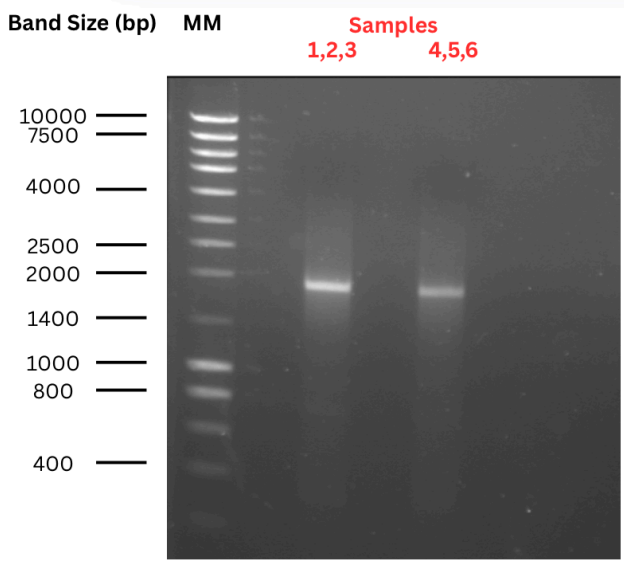

Figure 3.3: Agarose gel electrophoresis following restriction enzyme digestion of PCR products Six digestion reactions were performed, with samples loaded in two groups: samples 1-3 and samples 4-6. The DNA ladder in the first lane provides size reference, with bands ranging from 400 to 10,000 bp. The target DNA band with a size of 1882 bp is visible in lanes 3 and 5. The presence of clear, distinct bands allowed excision of the target fragment for subsequent purification.

The target band was excised and purified using the NZYTech Gel and PCR Purification Kit.

Following purification, DNA concentration was measured using a NanoDrop, yielding 16 ng/µL.

3.3 Ligation and Transformation

Bacterial transformation was confirmed by the presence of colonies on experimental plates. Colonies were observed on all experimental plates, confirming effective ligation and transformation.

- Both 1:1 and 1:5 molar ratio ligations yielded colonies, demonstrating effective insertion of the target DNA into the plasmid.
- No colonies were observed on the negative control plate, confirming the absence of self-ligation.

These results confirm that the ligation and transformation steps were effective, and colony screening can proceed to verify the presence of the correct insert.

3.4 Colony Screening

Colonies from the LB + Amp plates were screened to confirm the presence of the ligated construct. A matrix plate was created and the colonies were picked using sterile tips and resuspended directly in PCR tubes as the DNA template.

Following colony screening, 16 samples were analyzed via PCR to confirm the presence of the ligated insert. The agarose gel electrophoresis results identified five strong bands at the expected size (~2000 bp):

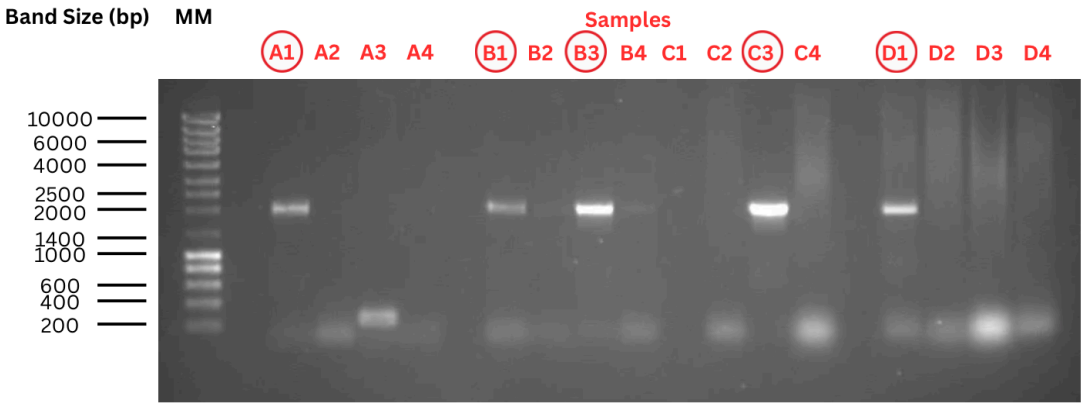

Figure 3.4: PCR screening of colonies selected from LB + Amp plates to confirm the presence of the ligated insert. The agarose gel displays PCR products, with five colonies (A1, B1, B3, C3, D1) exhibiting strong bands at approximately 2,000 bp, consistent with the expected size of the ligated insert.

- Clones (A1, B1, B3, C3, D) show expected bands sized to be 1882 bp
- These colonies were selected for overnight liquid culture at 30°C to prepare for plasmid purification (mini-prep).

Evaluation of Initial Sequencing Results

After performing mini-prep and sending A1, B1, B3, C3, and D1 for sequencing, the results indicated:

- A1 showed excessive recombination, suggesting an incorrect or altered insert.

- B1, B3, C3, and D1 were mostly correct, but sequencing noise suggested the possible presence of multiple sequences in some samples.

To ensure accuracy, an additional PCR was prepared:

- 8 PCR tubes total
    - 4 using mini-prep DNA (diluted 1:100)
    - 4 using the same colony cells directly from the plate

Agarose gel electrophoresis confirmed amplification of the expected fragment (~2000 bp) (Figure 3.5).

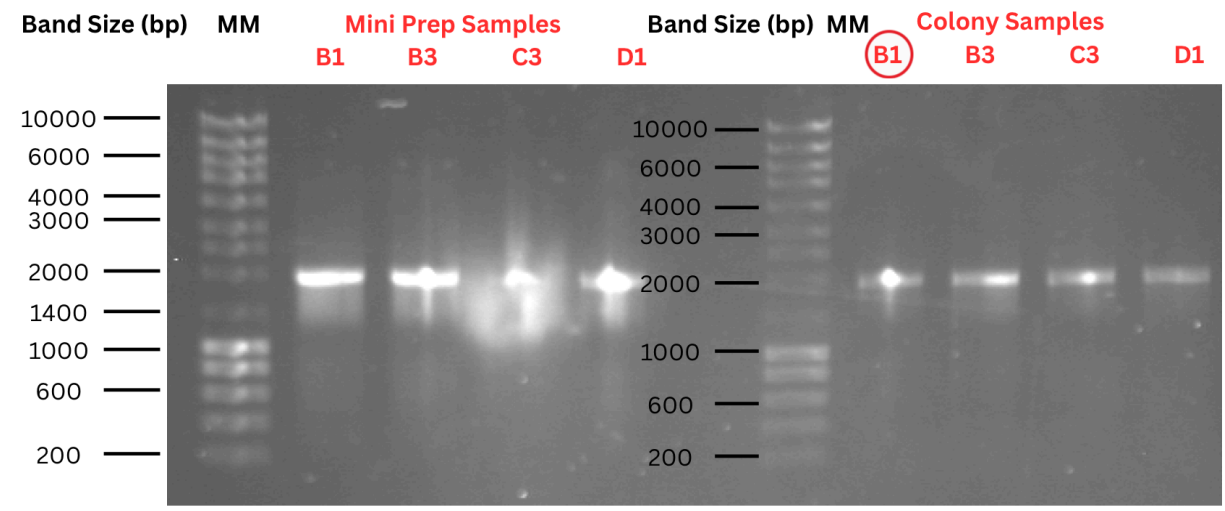

Figure 3.5: Agarose gel electrophoresis of the additional PCR amplifications performed on mini-prep DNA and directly from colonies to validate the presence of the expected insert (~2000 bp).

These results support the next step of forward and reverse sequencing to verify the integrity and correctness of the inserted sequence in the selected colonies.

3.5 Final Sequencing Results

To assess the sequence of zebrafish BiP (zfBiP) constructs, nucleotide sequence alignment was performed between two variants: Sequence_1 (ORF zfBiP_M1_pTrcHis.xdna) and Sequence_2 (zf_BiP_B1-FW_last.xdna) shown in the appendix.

The sequencing results obtained from both universal forward (FW) and reverse (RV) primers annealing upstream and downstream the insert were aligned and analyzed to identify nucleotide variations between Seq_1 (expected sequence) and Seq_2 from clone B1. The alignments revealed a 99.73% identity, with twelve different nucleotides across the 1882 base pairs of the insert. While the majority of these mutations were silent, preserving the original amino acid sequence due to the redundancy of the genetic code, two specific codons—codon 339 and codon 378—underwent missense mutations, resulting in amino acid changes.

- Codon 339: The expected codon CCG encoding proline was changed into CTG coding for a leucine.
- Codon 378: The expected codon CCT coding to a proline was changed into CTT coding for a leucine.

These differences were observed consistently in both FW (Appendix 5.1) and RV (Appendix 5.2) sequencing data, confirming their certainty and eliminating potential sequencing errors.

These missense mutations point to possible structural or functional changes on the expressed protein, depending on the role of these residues in its folding, stability, or interaction with other biomolecules. Further structural and functional analyses are required to assess the biological impact of these variations.

Since the PCR product was sequenced before ligation and transformation (data not shown) and at least the mutation on codon 339 was already present, this mutation may reveal a new BiP variant or may be attributed to polymerase errors despite the use of an error-proof DNA polymerase. Given the role of BiP as an ATPase-dependent chaperone involved in protein folding in the ER, these variations warrant further investigation to determine their impact on chaperone activity. Additional analyses, such as protein expression validation and functional assays, will be conducted to assess the biochemical implications of these differences.

3.6 ATPase Activity Assay

ATP hydrolysis was selected as an assay to address BiP functionality (the so-called BiP ATPase activity). The inorganic phosphate released by ATP hydrolysis catalyzed by BiP was quantified through the malachite green assay. The BiP from golden hamster available in the laboratory was

used as standard to evaluate the accuracy of the method and later on to compare with the ATPase activity of zebrafish BiP. Since BiP ATPase activity is dependent on the interaction with a J domain protein (Misselwitz et al., 1999), a generic protein fused to a consensus J domain (HaloTag-J domain) was thermally aggregated and used as BiP substrate (Melo et al., 2022). The standard curve for the ATPase assay is shown in Figure 3.6 and the BiP ATPase activity for 0.5 mM ATP is shown in Figure 3.7.

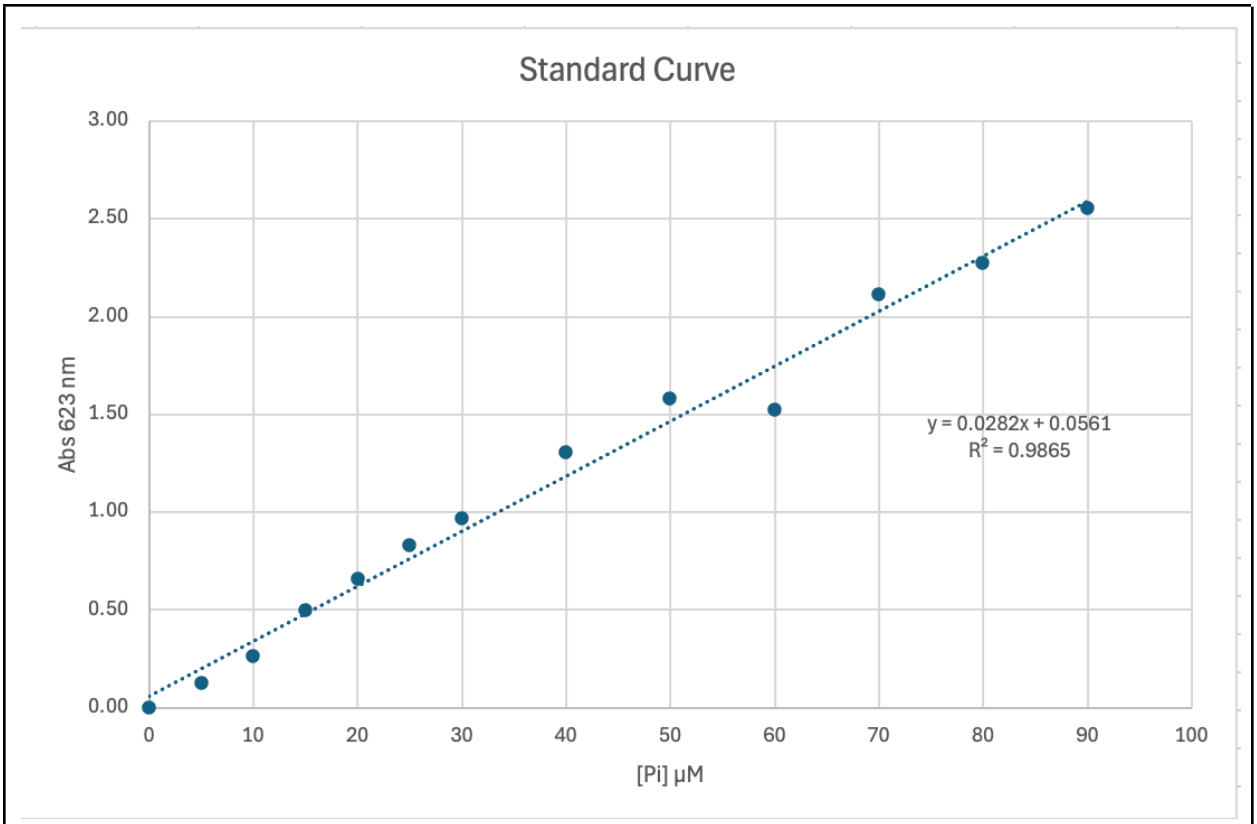

Figure 3.6: Standard curve generated from increasing concentrations of inorganic phosphate (Pi) and their absorbance at 623 nm. The linear fit shows a strong correlation (R^2 = 0.9865), with linearity up to 90 µM Pi, confirming the validity of the method for quantifying Pi released during ATP hydrolysis.

The method shows linearity up to 90 µM of inorganic phosphate (Pi) and a good correlation coefficient. Golden hamster BiP ATPase activity in the presence of 0.5 mM ATP was measured to be 51.4 µM/h as shown in figure 3.7.

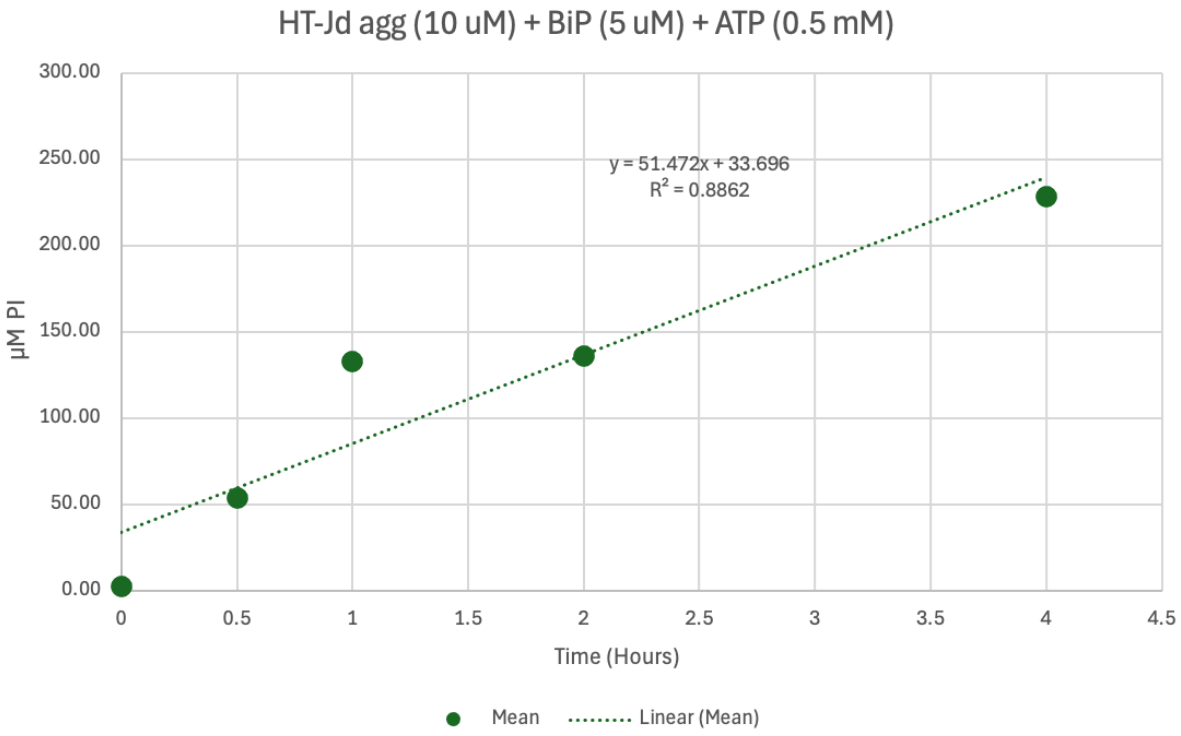

Figure 3.7 Time-dependent release of inorganic phosphate (Pi) in a reaction containing aggregated HT-Jd (10 µM), BiP (5 µM), and ATP (0.5 mM). The reaction displayed a linear increase in Pi release over 4 hours ($R^2 = 0.8862$), with a calculated rate of 51.47 µM Pi/h, representing BiP ATPase activity under these experimental conditions.

BiP ATPase activity remained linear throughout the four-hour assay, with a final calculated rate of 51.47 µM Pi per hour (Figure 3.7). This assay will subsequently be applied to evaluate the ATPase activity of zebrafish BiP.

Conclusion

ATPase-dependent chaperones, such as BiP, play central roles in facilitating protein folding, preventing aggregation, and mediating the disaggregation of misfolded polypeptides — functions that are particularly critical under conditions of cellular stress and in the pathophysiology of neurodegenerative diseases.

Using zebrafish as a vertebrate model offers a valuable comparative framework to study chaperone biology due to the evolutionary conservation of key protein homeostasis mechanisms. In this work, we successfully cloned the open reading frame (ORF) of zebrafish BiP (*Danio rerio*) into a pTrcHis-A vector for recombinant expression in *E. coli*. Cloning strategy included the omission of N-terminal sequence encoding the signal peptide that directs BiP to the ER, useless for the heterologous expression in *E. coli*. The construct was verified by sequencing.

The availability of recombinant zebrafish BiP soon enables a systematic comparison with orthologous chaperones from other species, such as golden hamster BiP, whose structural and functional properties have been well-characterized. This comparative approach will be crucial for delineating species-specific features versus conserved mechanistic functions in ER chaperone activity.

Moreover, this study sets the stage for detailed investigations into the disaggregase potential of zebrafish BiP, both independently and in coordination with co-chaperones. Given the critical role of protein aggregation in neurodegenerative disorders such as Alzheimer's, Parkinson’s, and ALS, a better understanding of how ER-resident chaperones contribute to aggregate clearance is of considerable biomedical interest.

In conclusion, the cloning of zebrafish BiP represents an essential first step toward elucidating the mechanistic basis of ER chaperone-mediated disaggregation. Future studies should quantify its ATP-dependent disaggregase activity, evaluate its capacity to solubilize disease-relevant protein aggregates, and directly compare its functional efficiency with mammalian orthologs. These investigations will provide valuable insights into the evolutionary conservation of chaperone function and may guide the development of therapeutic strategies aimed at enhancing proteostasis in neurodegenerative diseases.

5. Appendix

5.1 Alignment of Sequence_1: [ORF zfBiP_M1_pTrcHis.xdna] with Sequence_2: [zf_BiP_B1-FW_last.xdna] Forward Primer

Similarity : 1108/1111 (99.73 %)

```
Seq_1 1 atgggggttctcatcatcatcatcatggtatggctagcgttgggacagtgattggg 60
        ||||||||||||||||||||||||||||||||||||||||||||||||||||||||||||
Seq_2 1 ATGGGGGGTTCTCATCATCATCATCATGGTATGGCTAGCGTTGGGACAGTGATTGGG 60
Seq_1 61 atcgacctcgggaccacatactcctgtgttggagtctacaagaatggccgtgttgagatt 120
         |||||||| ||||||||||||||||||||||||||||||||||||||||||||||||||
Seq_2 61 ATCGACCTTGGGACCACATACTCCTGTGTTGGAGTCTACAAGAATGGCCGTGTTGAGATT 120
Seq_1 121 attgccaatgaccagggaaaccgcatcactccgtcatacgtggcctttaccactgaagga 180
          |||||||||||||||||||||||||||||||||||||| ||||||||||||||||||
Seq_2 121 ATTGCCAATGACCAGGGAAACCGCATCACTCCGTCATACGTAGCCTTTACCACTGAAGGA 180
Seq_1 181 gagcggctcatcggagatgctgcgaagaaccagctcacatccaaccctgaaaacactgtg 240
          ||||||||||||||||||||||||||||||||||||||||||||||||||||||||||||
Seq_2 181 GAGCGGCTCATCGGAGATGCTGCGAAGAACCAGCTCACATCCAACCCTGAAAACACTGTG 240
Seq_1 241 tttgacgccaagaggctgatcggacgcacatggggcgactcttctgtgcagcaggacatc 300
          ||||||||||||||||||||||||||||||||||||||||||||||||||||||||||||
Seq_2 241 TTTGACGCCAAGAGGCTGATCGGACGCACATGGGGCGACTCTTCTGTGCAGCAGGACATC 300
Seq_1 301 aaatacttccccttaaggtgatcgagaagaaaaacaagcctcacatccagctggacatc 360
          ||||||||||||||||||||||||||||||||||||||||||||||||||||||||||||
Seq_2 301 AAATACTTCCCCTTTAAGGTGATCGAGAAGAAAAACAAGCCTCACATCCAGCTGGACATC 360
Seq_1 361 ggctctggtcagatgaagacgtttgcaccggaggaaatttccgccatggttttgaccaag 420
          ||||||||||||||||||||||||||||||||||||||||||||||||||||||||||||
Seq_2 361 GGCTCTGGTCAGATGAAGACGTTTGCACCGGAGGAAATTTCCGCCATGGTTTTGACCAAG 420
Seq_1 421 atgaaggaaaccgcagaggcttatctgggaaagaaggtcactcatgctgtggtcaccgtt 480
          |||||||||||||||||||||| ||||||||||||||||||||||||||||||||||||
Seq_2 421 ATGAAGGAAACCGCAGAGGCTTACCTGGGAAAGAAGGTCACTCATGCTGTGGTCACCGTT 480
Seq_1 481 cctgcttatttcaacgatgctcagcgtcaggccactaaagatgctggaaccattgctggg 540
          ||||||||||||||||||||||||||||||||||||||||||||||||||||||||||||
Seq_2 481 CCTGCTTATTTCAACGATGCTCAGCGTCAGGCCACTAAAGATGCTGGAACCATTGCTGGG 540
Seq_1 541 ctgaatgtcatgaggatcatcaatgagcctacggcggctgccattgcatacggtctggac 600
          |||||||||||||||||||||||||||||||||||||||||||| ||||||||||||||||
Seq_2 541 CTGAATGTCATGAGGATCATCAATGAGCCTACGGCGGCTGCCATCGCATACGGTCTGGAC 600
Seq_1 601 aagagggacggagagaaaaacatcctggtgttcgatctgggtggtggcacctttgacgtg 660
          ||||||||||||||||||||||||||||||||||||||||||||||||||||||||||||
Seq_2 601 AAGAGGGACGGAGAGAAAAACATCCTGGTGTTCGATCTGGGTGGTGGCACCTTTGACGTG 660
Seq_1 661 tctctgctgaccatcgataacggcgtgtttgaagtggtggccacaaacggagacactcac 720
          ||||||||||||||||||||||||||||||||||||||||||||||||||||||||||||
Seq_2 661 TCTCTGCTGACCATCGATAACGGCGTGTTTGAAGTGGTGGCCACAAACGGAGACACTCAC 720
Seq_1 721 ctgggcggagaagacttcgaccagcgcgtcatggagcacttcatcaagctgtacaagaag 780
          ||||||||||||||||||||||||||||||||||||||||||||||||||||||||||||
Seq_2 721 CTGGGCGGAGAAGACTTCGACCAGCGCGTCATGGAGCACTTCATCAAGCTGTACAAGAAG 780
Seq_1 781 aagacgggcaaagacgtgcgcaaagacaaccgcgccgtgcagaagctgcgcagagaggtg 840
          ||||||||||||||||||||||||||||||||||||||||||||||||||||||||||||
```

```
Seq_2 781 AAGACGGGCAAAGACGTGCGCAAAGACAACCGCGCCGTGCAGAAGCTGCGCAGAGAGGTG 840
Seq_1 841 gagaaggctaagagagcgctgtctgcccagcatcaggcccgcatcgagatcgagtccttc 900
          ||||||||||||||||||||||||||||||||||||||||||||||||||||||||||||
Seq_2 841 GAGAAGGCTAAGAGAGCGCTGTCTGCCCAGCATCAGGCCCGCATCGAGATCGAGTCCTTC 900
Seq_1 901 tttgaaggagaagatttctctgagactctcaccagagccaagtttgaggagctcaacatg 960
          ||||| ||||||||||||||||||||||||||||||||||||||||||||||||||||||
Seq_2 901 TTTGAGGGAGAAGATTTCTCTGAGACTCTCACCAGAGCCAAGTTTGAGGAGCTCAACATG 960
Seq_1 961 gacttgttccgctccactatgaagccggttcagaaggttctggaggactctgacccgaag 1020
Seq_2 961 |||||||||||||||||||||||||||||||||||||||||||||||||||||| ||||
          GACTTGTTCCGCTCCACTATGAAGCCGGTTCAGAAGGTTCTGGAGGACTCTGACCTGAAG 1020
Seq_1  1021  aagccagatatcgatgagatcgtgctggtcggcggctccactcgtatcccgaagatccag  1080
          |||||||||||| |||||||||||| ||||||||||||||||||||||||||||||||||
Seq_2 1021 AAGCCAGATATTGATGAGATCGTGTTGGTCGGCGGCTCCACTCGTATCCCGAAGATCCAG 1080
Seq_1 1081 cagctggtgaaggagttcttcaacggaaaagagccgtccagaggaatcaaccctgacgag 1140
          |||||||||||||||||||| ||||||
Seq_2 1081 CAGCTGGTGAAGGAGTTCTTCA-TGGAAAA----------------------------- 1109
```

5.2 Alignment of Sequence_1: [ORF zfBiP_M1_pTrcHis.xdna] with Sequence_2: [zf_BiP_pTrcHis_B1+pBAD-R_last.ab1.xdna] Reverse Primer

Similarity : 1002/1004 (99.80 %)

```
Seq_1 901 tttgaaggagaagatttctctgagactctcaccagagccaagtttgaggagctcaacatg 960
                              ||||||||||||||||||||||||||||||||||||||
Seq_2  1044  --------------------GAGACTCTCACCAGAGCCAAGTTTGAGGAGCTCAACATG  1006
Seq_1 961  gacttgttccgctccactatgaagccggttcagaaggttctggaggactctgacccgaag 1020
           |||||||||||||||||||||||||||||||||||||||||||||||||||||||| ||||
Seq_2 1005 GACTTGTTCCGCTCCACTATGAAGCCGGTTCAGAAGGTTCTGGAGGACTCTGACCTGAAG 946
Seq_1 1021 aagccagatatcgatgagatcgtgctggtcggcggctccactcgtatcccgaagatccag 1080
           |||||||||||| |||||||||||| ||||||||||||||||||||||||||||||||||
Seq_2 945  AAGCCAGATATTGATGAGATCGTGTTGGTCGGCGGCTCCACTCGTATCCCGAAGATCCAG 886
Seq_1 1081 cagctggtgaaggagttcttcaacggaaaagagccgtccagaggaatcaaccctgacgag 1140
           |||||||||||||||||||||||| |||||||||||||||||||||||||||||| |||||||
Seq_2 885  CAGCTGGTGAAGGAGTTCTTCAATGGAAAAGAGCCGTCCAGAGGAATCAACCTTGACGAG 826
Seq_1 1141 gccgtggcgtacggagctgctgtccaggctggagtcctgtccggagaggaggagaccggt 1200
           ||||||||||||||||||||||||||||||||||||||||||||||||||||||||||||||
Seq_2 825  GCCGTGGCGTACGGAGCTGCTGTCCAGGCTGGAGTCCTGTCCGGAGAGGAGGAGACCGGT 766
Seq_1 1201 gatctggttcttctggacgtgtgtccgctgactctgggcattgagactgttggaggagtg 1260
           ||||||||||||||||||||||||||||||||||||||||||||||||||||||||||||||
Seq_2 765  GATCTGGTTCTTCTGGACGTGTGTCCGCTGACTCTGGGCATTGAGACTGTTGGAGGAGTG 706
Seq_1 1261 atgaccaaactcattcccagaaacactgttgttcccaccaagaaatcccagatcttctcc 1320
           ||||||||||||||||||||||||||||||||||||||||||||||||||||||||||||||
Seq_2 705  ATGACCAAACTCATTCCCAGAAACACTGTTGTTCCCACCAAGAAATCCCAGATCTTCTCC 646
Seq_1 1321 actgcttccgacaaccagcccaccgtcactatcaaagtttatgagggcgagcgtcccctg 1380
           ||||||||||||||||||||||||||||||||||||||||||||||||||||||||||||||
Seq_2 645  ACTGCTTCCGACAACCAGCCCACCGTCACTATCAAAGTTTATGAGGGCGAGCGTCCCCTG 586
Seq_1 1381 accaaagacaaccatctgctgggcacctttgacctgacaggcatccctccagcacctcgt 1440
           |||||||||||||||||||||||||||||||||||| ||||||||||||||||||||
Seq_2 585  ACCAAAGACAACCATCTGCTGGGCACCTTTGACCTGACTGGCATCCCTCCAGCACCTCGT 526
```

```
Seq_1 1441 ggtgtcccacagatcgaggtaactttcgagatcgacgtcaacggcatcctgcgcgtcacc 1500
           || ||||||||||||||||||||||||||||||||||||||||||||||||||||||||||
Seq_2 525  GGCGTCCCACAGATCGAGGTAACTTTCGAGATCGACGTCAACGGCATCCTGCGCGTCACC 466
Seq_1 1501 gccgaagacaaaggcaccggaaacaaaaacaagatcaccattaccaacgaccagaaccgg 1560
           ||||||||||||||||||||||||||||||||||||||||||||||||||||||||||||
Seq_2 465  GCCGAAGACAAAGGCACCGGAAACAAAAACAAGATCACCATTACCAACGACCAGAACCGG 406
Seq_1 1561 ctgacccctgaggacatcgagagaatggtgaacgaagccgagagattcgctgatgaggac 1620
           ||||||||||||||||||||||||||||||||||||||||||||||||||||||||||||
Seq_2 405  CTGACCCCTGAGGACATCGAGAGAATGGTGAACGAAGCCGAGAGATTCGCTGATGAGGAC 346
Seq_1 1621 aagaaactgaaggagagaatcgacagccgcaatgaattggagagctacgcctattccctg 1680
           ||||||||||||||||||||||||||||||||||||||||||||||||||||||||||||
Seq_2 345  AAGAAACTGAAGGAGAGAATCGACAGCCGCAATGAATTGGAGAGCTACGCCTATTCCCTG 286
Seq_1 1681 aagaaccagatcggggataaagagaaattaggcggaaagttatcctctgaagacaaggag 1740
           |||||||||||||||||||||||||||||| ||||||||||||||||||||||||||||
Seq_2 285  AAGAACCAGATCGGGGATAAAGAGAAATTAGGTGGAAAGTTATCCTCTGAAGACAAGGAG 226
Seq_1 1741 gccatcgagaaggcagtggaggagaagatcgagtggctggaggcgcatcaggacgccgat 1800
           ||||||||||||||||||||||||||||||||||||||||||||||||||||||||||||
Seq_2 225  GCCATCGAGAAGGCAGTGGAGGAGAAGATCGAGTGGCTGGAGGCGCATCAGGACGCCGAT 166
Seq_1 1801 ctggaggaattccaggccaaaaagaaggagctggaggaggtggtgcagcccatcgtcagc 1860
           ||||||||||||||||||||||||||||||||||||||||||||||||||||||||||||
Seq_2 165  CTGGAGGAATTCCAGGCCAAAAAGAAGGAGCTGGAGGAGGTGGTGCAGCCCATCGTCAGC 106
Seq_1 1861 aaactgtacggcagtgcgggaggaccaccgcctgaagaggccgaagagaaggacgagctg 1920
           ||||||||||||||||||||||||||||||||||||||||||||||||||||||||||||
Seq_2 105  AAACTGTACGGCAGTGCGGGAGGACCACCGCCTGAAGAGGCCGAAGAGAAGGACGAGCTG 46
Seq_1 1921 tag---------------------------------------- 1923
           |||
Seq_2 45   TAGGGATCCGAGCTCGAGATCTGCAGCTGGTACCATATGGGAATT 1
```

References

Amsterdam A, Lin S, Hopkins N. 1995. The *Aequorea victoria* green fluorescent protein can be used as a reporter in live zebrafish embryos. *Dev Biol.* 171(1):123–129. doi:10.1006/dbio.1995.1265

Audouard C, Masson F, Charry C, Li Z, Christians E. 2011. Oocyte-targeted deletion reveals that Hsp90b1 is needed for the completion of first mitosis in mouse zygotes. *PLoS One.* 6(2):e17109. doi:10.1371/journal.pone.0017109

Behnke J, Feige MJ, Hendershot LM. 2015. BiP and its nucleotide exchange factors Grp170 and Sil1: mechanisms of action and biological functions. *J Mol Biol.* 427(7):1589–1608. doi:10.1016/j.jmb.2015.02.010

Bohush A, Bieganowski P, Filipek A. 2019. Role of molecular chaperones in protein misfolding diseases. *Int J Mol Sci.*20(22):6146. doi:10.3390/ijms20226146

Bross P, Fernandez-Guerra P, Usselman RJ. 1999. Molecular chaperones and their role in proteostasis. *FEBS Lett.*451(1):1–8.

Bulic B, Pickhardt M, Schmidt B, Mandelkow E. 2011. Small molecule inhibitors of tau aggregation: targeting the root of Alzheimer's disease. *Biochim Biophys Acta Mol Basis Dis.* 1812(4):427–438.

Ciechanover A, Kwon YT. 2017. Protein quality control by molecular chaperones in neurodegeneration. *Cell.*171(5):1026–1038. doi:10.1016/j.cell.2017.10.026

Faye MD, McCarthy-Culpepper C, Sargueil B. 2019. Structural dynamics of BiP during the ATPase cycle. *J Biol Chem.*294(9):3337–3348.

Galbreath EJ, et al. 2013. Genetic susceptibility and therapeutic strategies in neurodegenerative diseases. *Brain Res Bull.*98:48–58.

Galván A, Wichmann T. 2008. Pathophysiology of parkinsonism. *Clin Neurophysiol.* 119(7):1459–1474. doi:10.1016/j.clinph.2008.03.017

Gorbatyuk M, Gorbatyuk O. 2013. The molecular chaperone GRP78/BiP as a therapeutic target for neurodegenerative diseases. *Front Neurosci.* 7:125. doi:10.3389/fnins.2013.00125

Griffith R, Holmes J. 2019. The HSP family: protein folding, disease and aging. *Annu Rev Biochem.* 88:991–1019.

Guo T, Noble W, Hanger DP. 2017. Roles of tau protein in health and disease. *Acta Neuropathol.* 133(5):665–704. doi:10.1007/s00401-017-1707-9

Hiller MM, Burmann BM. 2018. The significance of ATPase-dependent chaperones in protein homeostasis. *Nat Rev Mol Cell Biol.* 19(11):715–732.

Hoshino T, et al. 2011. Suppression of Alzheimer's disease-related phenotypes by expression of heat shock proteins: a molecular chaperone approach. *Proc Natl Acad Sci USA.* 108(9):4125–4130.

Imbimbo BP, Lombard J, Pomara N. 2005. Pathophysiology of Alzheimer's disease: from amyloid-beta to neurodegeneration. *Ageing Res Rev.* 4(2):153–177.

Jellinger KA. 2010. Pathology and pathogenesis of neurodegenerative disorders. *Acta Neuropathol.* 119(1):1–20. doi:10.1007/s00401-009-0620-0

Jin Y, Awad W, Petrova K, Hendershot LM. 2017. The BiP chaperone cycle: mechanism and function in ER protein homeostasis. *J Cell Sci.* 130(7):1340–1350.

Kim YE, Hipp MS, Bracher A, Hayer-Hartl M, Hartl FU. 2013. Molecular chaperone functions in protein folding and proteostasis. *Annu Rev Biochem.* 82:323–355.

Krone PH, Evans TG, Blechinger SR. 2003. Heat shock gene expression and function during zebrafish development. *Semin Cell Dev Biol.* 14(5):267–274.

Lackie RE, Maciejewski A, Ostapchenko VG. 2017. The Hsp70/Hsp90 chaperone machinery in neurodegenerative diseases. *Front Neurosci.* 11:254. doi:10.3389/fnins.2017.00254

Lee VM, Goedert M, Trojanowski JQ. 2010. Neurodegenerative tauopathies. *Annu Rev Neurosci.* 33:145–168. doi:10.1146/annurev-neuro-060909-153602

Lee JH, et al. 2020. Environmental effects on amyloid-beta aggregation and toxicity. *Neurobiol Dis.* 134:104646.

Li J, et al. 2022. Ubiquitin–proteasome system and autophagy in neurodegenerative disorders. *Biochim Biophys Acta Mol Basis Dis.* 1868(1):166339.

Lu RC, et al. 2014. The molecular chaperone network in neuronal health and disease. *Cell Mol Life Sci.* 71(18):3581–3598.

Maharaj R, et al. 2016. ATPase cycles of Hsp70 family members: conformational transitions and client release. *J Biol Chem.* 291(16):8532–8541.

Marzec M, Eletto D, Argon Y. 2011. GRP94: an HSP90-like protein specialized for protein folding and quality control in the endoplasmic reticulum. *Biochim Biophys Acta Mol Cell Res.* 1823(3):774–787.

Mathur M, Sutton S. 2017. Genetic insights into neurodegenerative diseases: from models to therapy. *Brain Sci.* 7(7):81. doi:10.3390/brainsci7070081

Maziuk B, Ballance HI, Wolozin B. 2017. Dysregulation of RNA binding protein aggregation in neurodegenerative diseases. *Front Mol Neurosci.* 10:89. doi:10.3389/fnmol.2017.00089

Moran L, et al. 2009. The role of Hsp70 in protein degradation and quality control. *FEBS J.* 276(20):5936–5949.

Morris M, et al. 2008. Amyloid-beta and tau interactions in Alzheimer's disease. *Nat Rev Neurosci.* 9(8):545–555.

Nakamura T, Lipton SA. 2010. Redox modulation of protein misfolding, mitochondrial dysfunction, synaptic damage, and cell death in neurodegenerative diseases. *Cell Res.* 20(3):293–305. doi:10.1038/cr.2010.10

Nogueira M, et al. 2018. Cooperation between Hsp70 and co-chaperones in protein disaggregation. *J Biol Chem.*293(48):18820–18832.

Ormandy GC, et al. 2011. Transgenic animal models for neurodegenerative disease research. *Brain Res Bull.* 87(1):20–29.

Ortbauer M. 2013. Environmental parameters affecting protein aggregation: pH, temperature, and ionic strength. *Biophys Chem.* 181:14–20.

Perri ER, et al. 2016. Tauopathies and protein aggregation diseases. *Mol Neurobiol.* 53(10):6825–6846.

Pobre KFR, Poet GJ, Hendershot LM. 2018. The endoplasmic reticulum chaperone BiP is a master regulator of ER function. *Front Mol Biosci.* 5:16. doi:10.3389/fmolb.2018.00016

Rios P, Barducci A. 2014. Structural dynamics of Hsp70 during ATP hydrolysis and substrate release. *Biophys J.*106(8):1752–1762.

Ruffini N, et al. 2020. Genetic factors in neurodegenerative diseases associated with protein aggregation. *Neurobiol Dis.*138:104792.

Saibil H. 2013. Chaperone machines for protein folding, unfolding and disaggregation. *Nat Rev Mol Cell Biol.*14(10):630–642.

Schaffert LN, Carter WG. 2020. Do post-translational modifications influence protein aggregation in neurodegenerative diseases? *Brain Res.* 1739:146–153. doi:10.1016/j.brainres.2020.146823

Sierra-Fonseca JA, Gosselink KL. 2018. Tau phosphorylation and neurodegeneration: the role of stress-activated kinases. *Front Neurosci.* 12:698. doi:10.3389/fnins.2018.00698

Sottile V, Nadin S. 2017. Heat shock proteins in development and aging. *Cell Stress Chaperones.* 22(4):539–548.

Soto C, Satani N. 2010. The intricate mechanisms of amyloid aggregation: relevance to neurodegenerative diseases. *J Neurochem.* 116(1):1–12.

Turturici G, et al. 2011. Hsp70 and synaptic function: roles in neuronal plasticity. *Front Biosci.* 16:268–283.

Ullman MT. 2013. Contributions of memory systems to language: evidence from neuroimaging and disorders. *Trends Cogn Sci.* 17(10):618–628.

Wareham LK, et al. 2022. Targeting protein misfolding and aggregation in neurodegenerative diseases. *Nat Rev Drug Discov.* 21(8):611–633.

Wang Y. 2005. α-Synuclein and its role in Parkinson's disease. *Mol Neurobiol.* 31(3):273–284.

Wang M, Kaufman RJ. 2017. Protein misfolding in the endoplasmic reticulum as a conduit to human disease. *Nature.*529(7586):326–335.

Wentink A, et al. 2020. Molecular dissection of protein disaggregation by human Hsp70 chaperones. *Nature.*587(7834):483–488.

Zampar GG, et al. 2024. Synucleinopathies: mechanisms of α-synuclein aggregation and neurotoxicity. *Prog Neurobiol.*233:102131.

Zhou C, et al. 2022. Pathological protein aggregation and neurodegeneration. *Mol Neurodegener.* 17(1):33.